AD-A105 928 COLORADO UNIV AT BOULDER ELECTROMAGNETICS LAB F/G 9/3
RADIATION LOSS FROM A CURVED DIELECTRIC CHANNEL WAVEGUIDE IN A --ETC(U)
JUN 81 E F KUESTER, R J HOLLAND, D C CHANG DAAG29-78-6-0173
UNCLASSIFIED SCIENTIFIC-64 ARO-15632.5-EL NL

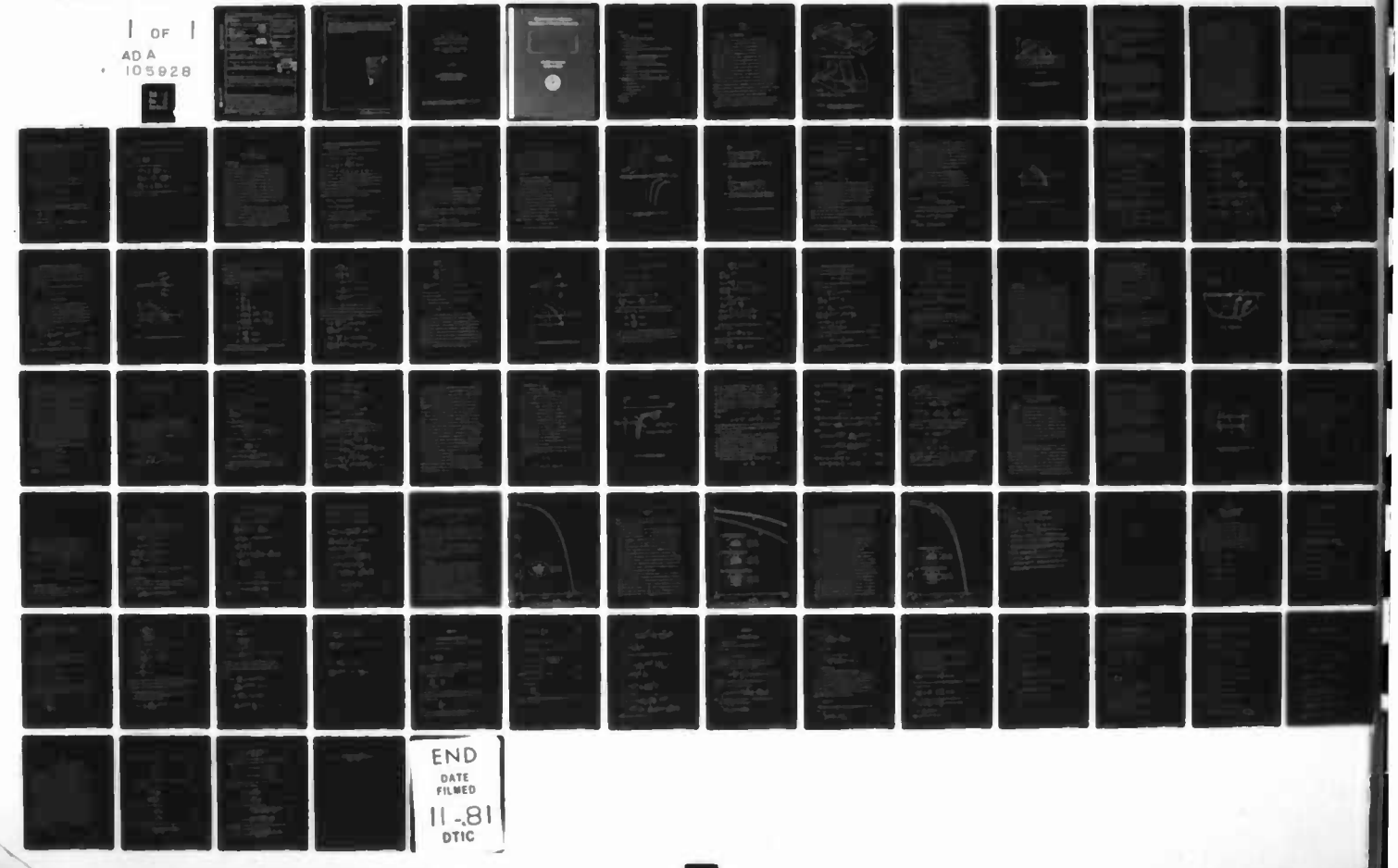


A
59

REPORT DOCUMENTATION PAGE

READ INSTRUCTIONS BEFORE COMPLETING FORM

1. REPORT NUMBER (19) 15632.5-EL	2. GOVT ACCESSION NO AD-A105928
3. RECIPIENT'S CATALOG NUMBER (8)	
4. TITLE (and Subtitle) (6) Radiation Loss from a Curved Dielectric Channel Waveguide in a Dense Substrate.	5. TYPE OF REPORT & PERIOD COVERED (9) Technical rept.
	6. PERFORMING ORG. REPORT NUMBER
7. AUTHOR(s) (10) Edward F. Kuester, Robert L. Holland, David C. Chang (15)	8. CONTRACT OR GRANT NUMBER(s) DAAG29-78-G-0173
9. PERFORMING ORGANIZATION NAME AND ADDRESS University of Colorado, Boulder, CO 80309	10. PROGRAM ELEMENT, PROJECT, TASK AREA & WORK UNIT NUMBERS (11)
11. CONTROLLING OFFICE NAME AND ADDRESS U. S. Army Research Office, Post Office Box 12211, Research Triangle Park, NC 27709	12. REPORT DATE Jun 81
	13. NUMBER OF PAGES 82
14. MONITORING AGENCY NAME & ADDRESS(if different from Controlling Office) (18) ARO (12) 86	15. SECURITY CLASS. (of this report) Unclassified
	15a. DECLASSIFICATION/DOWNGRADING SCHEDULE

16. DISTRIBUTION STATEMENT (of this Report)

Approved for public release; distribution unlimited.

(14) SCIENTIFIC-64

DTIC ELECTE OCT 21 1981 S D H

17. DISTRIBUTION STATEMENT (of the abstract entered in Block 20, if different from Report)

NA

18. SUPPLEMENTARY NOTES

The view, opinions, and/or findings contained in this report are those of the author(s) and should not be construed as an official Department of the Army position, policy, or decision, unless so designated by other documentation.

19. KEY WORDS (Continue on reverse side if necessary and identify by block number)

20. ABSTRACT (Continue on reverse side if necessary and identify by block number)

This report gives the results of an investigation to analytically determine the effect of a plane dielectric interface upon the radiation loss of a curved channel dielectric waveguide embedded in a dense substrate and bent in a plane parallel to that of the material interface. The radiation loss from bent dielectric waveguides is of interest for a variety of potential applications in integrated optics. Knowledge of the factors influencing the radiation from bend dielectric waveguides will allow the design of integrated optical component characteristics which, in

20. ABSTRACT CONTINUED

one application, may result in decreased radiation to conserve signal energy or which, in another application, may achieve enhanced radiation effects in order to optimize the coupling between vatious optical waveguides. An obvious example for which the conservation of signal energy is of prime concern is the dielectric fiber transmission line used in simple point-to-point data transfer applications.

Scientific Report No. 64

RADIATION LOSS FROM A CURVED DIELECTRIC CHANNEL WAVEGUIDE IN A DENSE SUBSTRATE

by

Edward F. Kuester, Robert L. Holland
and David C. Chang

June 1981

Electromagnetics Laboratory
Department of Electrical Engineering
University of Colorado
Boulder, Colorado 80309

This research was supported by the Army Research Office (ARO) under grant no. DAAG29-G-0173, monitored by Dr. J. Mink.

Electromagnetics Laboratory
Department of Electrical Engineering

UNIVERSITY OF COLORADO
BOULDER, COLORADO

TABLE OF CONTENTS

CHAPTER 1

Prologue

1.1 Study Objective and Methodology

The primary objective of this investigation was to analytically determine the effect of a plane dielectric interface upon the radiation loss of a curved channel dielectric waveguide embedded in a dense substrate and bent in a plane parallel to that of the material interface. The radiation loss from bent dielectric waveguides is of interest for a variety of potential applications in integrated optics. Knowledge of the factors influencing the radiation from bend dielectric waveguides will allow the design of integrated optical component characteristics which, in one application, may result in decreased radiation to conserve signal energy or which, in another application, may achieve enhanced radiation effects in order to optimize the coupling between vatious optical waveguides. An obvious example for which the conservation of signal energy is of prime concern is the dielectric fiber transmission line used in simple point-to-point data transfer applications. Examples of integrated optical components in which some specific level of radiation is desired include optical filters (e.g., ring resonator discriminators; cf. [1]) and optical directional couplers (cf. [2]). Figure 1.1 illustrates potential realizations of these latter components.

Arnaud (cf. [3]) has treated radiation loss from a slab-loaded, bent dielectric rod, and this structure is the one described in the literature that has the most in common with the configuration considered herein.

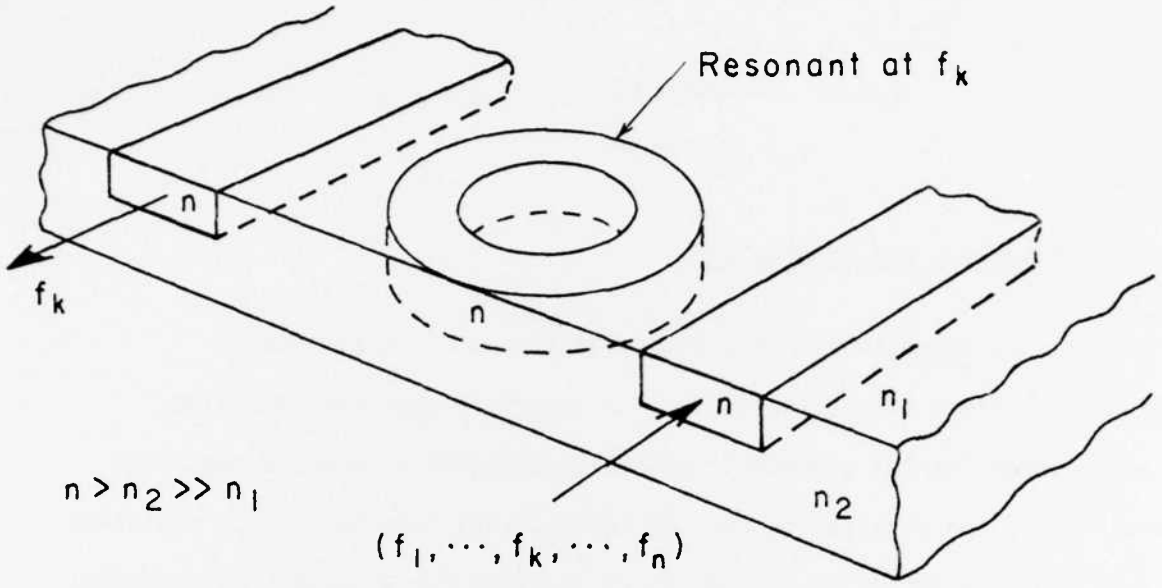

(a) A RING RESONATOR DISCRIMINATOR

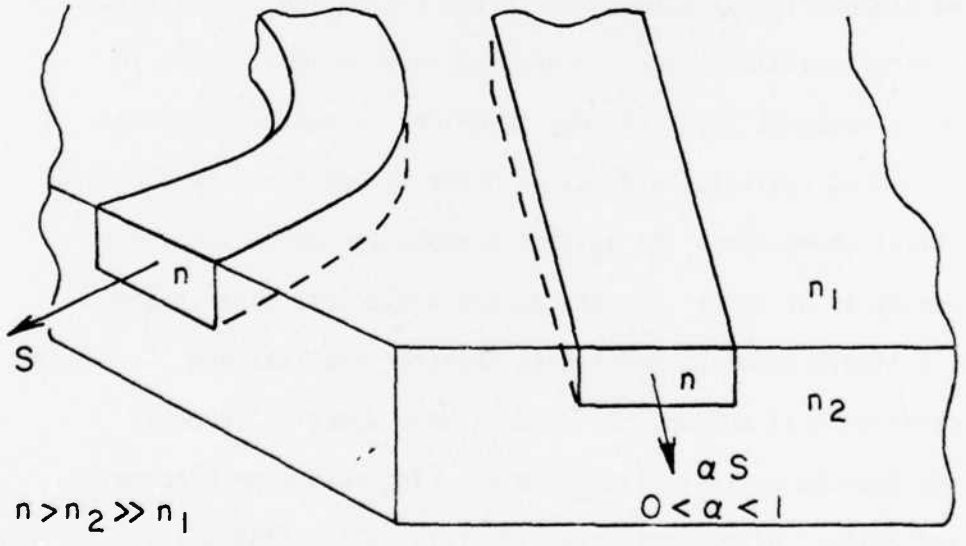

(b) A DIRECTIONAL COUPLER

Figure 1.1 Dielectric Channel Waveguides in Potential Integrated Optics Applications

However, primarily because of the finite extent of the slab and the fact that the refractive indices of the slab and the rod are equal, Arnaud's problem differs significantly from that discussed in this report. Indeed, the differences are substantial enough to preclude extensive corroboration of either study's results by direct comparison.

Figure 1.2 illustrates the fundamental geometry of the problem and depicts the coordinate reference frames chosen for the analysis. The refractive indices of the channel waveguide, the substrate material, and the covering material have the values n, n_2, and n_1, respectively. These refractive indices are ordered according to the relation $n > n_2 >> n_1$, the relation $n_2 >> n_1$ expressing what is meant by "dense" as applied to the substrate material. A global, circular-cylindrical reference frame with spatial coordinates r, ϕ, and z has its origin at the point 0, and a local cartesian reference frame with spatial coordinates x, y, and s has its origin at the point $(R_o, 0, 0)$ relative to the global frame. The extent of the channel waveguide is defined by the radial boundaries at r'' and r''' and by the coordinates $z = 0$ and $z = z''$, which define horizontal planes between which the guide is confined. The quantity Ro is given by the expression $R_o = (r' + r''')/2$ and is defined to be the radius of curvature of the channel waveguide.

A propagating mode with phase factor $\exp i(\omega t - k_o \gamma R_o \phi)$ is assumed to exist, where $k_o = \omega\sqrt{\mu_o \epsilon_o}$ is the free space propagation constant and γ is the normalized (to k_o), complex propagation constant of the mode in the curved channgel waveguide. Given that the normalized propagation constant for the straight channel waveguide is γ_o, the analysis proceeds to compute a first order representation of γ of the form

$$\gamma = \gamma_o - i\alpha , \quad \alpha > 0 \tag{1.1}$$

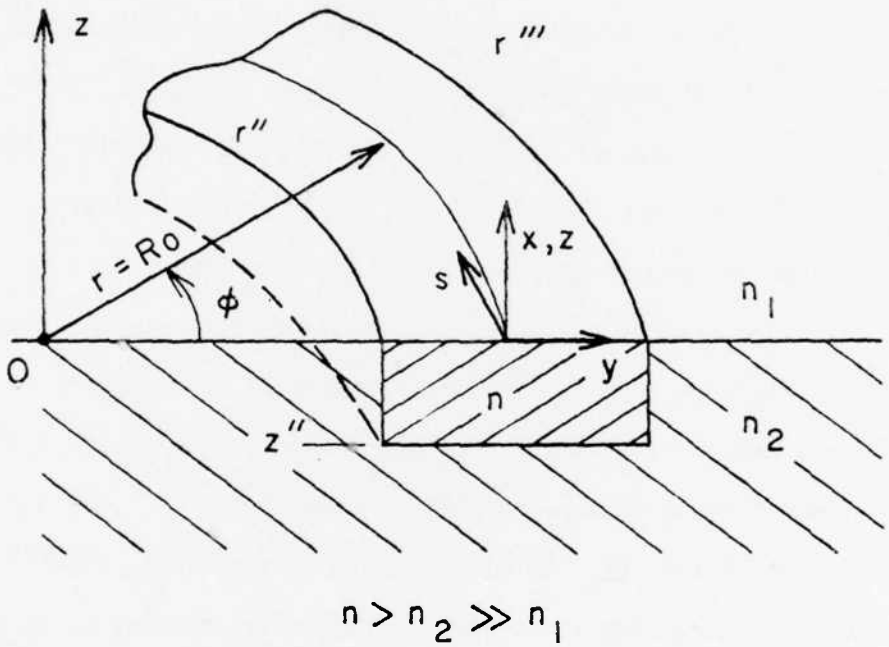

Figure 1.2 A Curved Channel Waveguide Embedded in a Dense Substrate

where α is the normalized attenuation coefficient of the mode. The mode attenuation due to continuous radiation from the bend following propagation through an angular sector ϕ of the channel guide is then given by the factor $\exp(-\alpha k_o R_o \phi)$.

Once α has been determined, the study objective is attained via a comparison of α with the normalized attenuation constant of a bent channel waveguide embedded in a homogeneous medium.

1.2 Summary of Results

The normalized attenuation constant α' of a bent, rectangular dielectric waveguide immersed in a nomogeneous medium has the general form [5]

$$\alpha' = \frac{C_h}{(k_o R_o)^{\frac{1}{2}}} e^{k_o R_o Q(0)}$$

where $C_n > 0$ and $Q(0) < 0$ are parameters depending upon material characteristics of the guide (including physical dimensions) and its surrounding medium as well as the specific mode assumed to be propagating in the guide. As a result of this investigation, the normalized attenuation constant α for the bent, rectangular dielectric waveguide embedded in a dense substrate below a material interface is found to be of the form

$$\alpha = \frac{C_i}{(k_o R_o)^{3/2}} e^{k_o R_o q_2(0)}$$

where $C_i > 0$ and $q_2(0) < 0$ depend upon the channel guide, substrate, and covering medium characteristics (including the physical dimensions of the guide) and upon the specific mode assumed to be propagating in the guide.

Three observations are of importance. First, the quantities C_h and C_i are in general unequal, as are $Q(0)$ and $q_2(0)$ (although a certain formal similarity between the latter two exists). Second, the fundamental exponential dependence of both α' and α on R_o is the same. Third, the algebraic dependence of α' and α on R_o is distinctly different. The $(\frac{1}{R_o})^{3/2}$ algebraic dependence of α upon R_o arises as the leading term of the asymptotic expansion of α and thus imparts a lateral wave characteristic (cf. 4, Section 5.5) to the radiation loss of a rectangular dielectric guide in a dense substrate below a material interface. Indeed, the absence of a $(\frac{1}{R_o})^{\frac{1}{2}}$ leading term in the asymptotic expansion of α may be thought of as resulting from the first order cancellation of source and image field due to the presence of the interface.

As a means of comparing the influence of the factors $\frac{C_h}{(k_oR_o)^{\frac{1}{2}}}$ and $\frac{C_i}{(k_oR_o)^{3/2}}$ on the radiation loss of their associated waveguiding structures, α' and α are plotted versus k_oR_o for bent, rectangular dielectric waveguides whose dimensions and/or refractive indices are chosen so that $Q(0) = q_2(0)$. This not only assures that the exponential variation with R_o will be the same in each case, but it also corresponds to a situation in which propagation constant along the central axis of each guide is the same. For the cases considered, α is found to be always less than α' and is, in particular, less than an order of magnitude smaller than α' for $k_oR_o = 500$ and between one and two orders of magnitude smaller than α' for $k_oR_o = 5000$. This indicates that one may in some instances achieve a significant reduction in the radiation loss of a bent, rectangular dielectric waveguide by embedding it below a high contrast dielectric interface in the material of greater refractive index.

1.3 Analytical Preliminaries

This report will not present a derivation of the general form of α, but will merely quote the result as given in [5], Chapter 9. Thus

$$\alpha = \frac{C}{k_0 P} \tag{1.2}$$

where

$$P = 2 \int \bar{a}_s \cdot \bar{E}_0 \times \bar{H}_0 ds \tag{1.3}$$

$$C = \int_{-\infty}^{\infty} \{\bar{E}_0^- \times \overline{\delta H} - \overline{\delta E} \times \bar{H}_0^-\} \cdot \bar{a}_y dz \Big|_{y=y_0} \tag{1.4}$$

In (1.3), the integration extends over an infinite plane containing a cross section of the channel waveguide, and y_0 is some point chosen outside the bend (beyond r''') of the curved channel guide where the fields have decayed sufficiently (cf.[2]). The fields $\bar{E}_0$ and $\bar{H}_0$ are those of the straight channel guide, and $\bar{E}_0^-$ and $\bar{H}_0^-$ are the fields of the straight channel traveling in the "negative" ϕ (or s)-direction. The fields $\overline{\delta E}$ and $\overline{\delta H}$ constitute that portion of the fields outside the curved channel guide which have been reflected from the caustic or turning point beyond which the mode must radiate in a radially outward direction. The fundamental analytical task of this investigation was that of expressing the fields $\overline{\delta E}$ and $\overline{\delta H}$ in terms of known quantities, i.e., in terms of $\bar{E}_0$, $\bar{H}_0$, γ_0, R_0, etc.

As a result of the circular-cylindrical symmetry of the global reference frame, our subsequent analysis will be facilitated by concentrating on the field components E_z and H_z, although we must eventually consider all of the field components. Via Maxwell's equations and standard

analysis for circular-cylindrical geometry, we find that we may express the four remaining field components in terms of E_z and H_z, whence

$$(k^2 + \frac{\partial^2}{\partial z^2}) E_\phi = i\zeta_o k_o \frac{\partial H_z}{\partial r} - i\gamma k_o \frac{R_o}{r} \frac{\partial E_z}{\partial z} \tag{1.5a}$$

$$(k^2 + \frac{\partial^2}{\partial z^2}) E_r = -\zeta_o \gamma k_o^2 \frac{R_o}{r} H_z + \frac{\partial^2}{\partial r \partial z} E_z \tag{1.5b}$$

$$(k^2 + \frac{\partial^2}{\partial z^2}) H_\phi = -\frac{i n^2}{\zeta_o} k_o \frac{\partial E_z}{\partial r} - i\gamma k_o \frac{R_o}{r} \frac{\partial Hz}{\partial z} \tag{1.5c}$$

$$(k^2 + \frac{\partial^2}{\partial z^2}) H_r = \frac{n^2}{\zeta_o} \gamma k_o^2 \frac{R_o}{r} E_z + \frac{\partial^2}{\partial r \partial z} H_z \tag{1.5d}$$

where $\zeta_o = \sqrt{\mu_o/\epsilon_o}$, $k^2 = n_1^2 k_o^2$ for $z > 0$, $k^2 = n_2^2 k_o^2$ for $z < 0$.

We will show in Chapter 2 that both E_z and H_z have Fourier-Bessel representations of the form

$$E_z(r,\phi,z) = e^{-i\nu\phi} \int_0^\infty \tilde{E}_z(\alpha,z) J_\nu(k_o \alpha r) \alpha d\alpha \tag{1.6a}$$

$$H_z(r,\phi,z) = e^{-i\nu\phi} \int_0^\infty \tilde{H}_z(\alpha,z) J_\nu(k_o \alpha r) \alpha d\alpha \tag{1.6b}$$

All of the desired field components have similar representations, and the z-variation is such as to yeild the following equivalence of operators

$$(\frac{\partial^2}{\partial z^2} + k^2) = k_o^2 \alpha^2 \tag{1.7}$$

for the field transforms.

For example, consider the electric field component E_ϕ given by

$$E_\phi = e^{-i\nu\phi} \int_0^\infty \tilde{E}_\phi(\alpha,z) J_\nu(k_o \alpha r) \alpha d\alpha \tag{1.8}$$

$\tilde{E}_\phi(\alpha,z)$ is the field transform of E_ϕ and $(\frac{\partial^2}{\partial z^2} + k^2)\tilde{E}_\phi(\alpha,z) = k_o^2\alpha^2\tilde{E}_\phi$.

Substitution of (1.6a), (1.6b), and (1.8) into (1.5a) and making use of (1.7) gives

$$\alpha^2\tilde{E}_\phi = i\zeta_o\alpha \frac{J_\nu'(k_o\alpha r)}{J_\nu(k_o\alpha_r)} \tilde{H}_z - \frac{i\gamma R_o}{rk_o} \frac{\partial}{\partial z}\tilde{E}_z . \tag{1.9a}$$

In a similar fashion we find the following as well:

$$\alpha^2\tilde{E}_r = -\frac{\zeta_o\gamma R_o}{r} \tilde{H}_z + \frac{\alpha}{k_o} \frac{J_\nu'(k_o\alpha r)}{J_\nu(k_o\alpha r)} \frac{\partial}{\partial z} \tilde{E}_z \tag{1.9b}$$

$$\alpha^2\tilde{H}_\phi = -\frac{i\gamma R_o}{rk_o} \frac{\partial}{\partial z}\tilde{H}_z - i\frac{\alpha n_{1,2}^2}{\zeta_o} \frac{J_\nu'(k_o\alpha r)}{J_\nu(k_o\alpha r)} \tilde{E}_z \tag{1.9c}$$

$$\alpha^2\tilde{H}_r = \frac{\gamma R_o n_{1,2}^2}{r\zeta_o} \tilde{E}_z + \frac{\alpha}{k_o} \frac{J_\nu'(k_o\alpha r)}{J_\nu(k_o\alpha r)} \frac{\partial}{\partial z} \tilde{H}_z \tag{1.9d}$$

The relationships (1.10a) through (1.10d) between the field (Fourier-Bessel) transforms will be of use in Chapter 2.

CHAPTER 2

INTEGRAL REPRESENTATIONS OF THE CARTESIAN FIELD COMPONENTS

2.1 Introduction

This chapter is devoted to finding integral representations for the Cartesian field components E_z and H_z. As mentioned in Chapter 1, knowledge of these allows one to determine the remaining four field components via (1.5a) through (1.5d). The components E_z and H_z are preferred by the circular-cylindrical geometry of our problem to the extent that they both satisfy the homogeneous (in source free regions), scalar wave equation, i.e., the Helmholtz equation. This fact, together with the assumed form of the field variation with the spatial coordinate ϕ, allows specification of the Fourier-Bessel transforms of E_z and H_z to within multiplicative factors which must be determined through the application of boundary and source conditions. Explicit evaluation of these is the subject of Section 2.3.

Although at first glance the final form of the integral representations of E_z and H_z seems too cumbersome for practical use due to the complexity of the required integrations, it will be seen in Chapter 3 that the integral representations derived in this chapter are amenable to asymptotic analysis when $k_o R_o >> 1$, i.e., when the radius of curvature of the bend channel guide is large relative to the wavelength of the propagating fields.

2.2 Extended Fourier-Bessel Representations for Field Solutions of the Helmholtz Equation

Let $F(r,\phi,z) = \Phi(r,z)e^{-i\nu\phi}$ be a scalar field satisfying the Helmholtz equation for source-free regions,

$(\nabla^2 + k^2)F(r,\phi,z) = 0$, then for $\nu = k_o\gamma R_o$,

$$\left\{\frac{1}{r}\frac{\partial}{\partial r}\, r\, \frac{\partial}{\partial r} + \frac{\partial^2}{\partial z^2} + k^2 - \frac{\gamma^2 k_o^2 R_o^2}{r^2}\right\} \Phi(r,z) = 0 \tag{2.1}$$

where, as before, $k^2 = n_1^2 k_o^2$ for $z > 0$, and $k^2 = n_2^2 k_o^2$ for $z < 0$. In this section, $\Phi(r,z)$ is a generic symbol representative of either $E_z(r,z)$ or $H_z(r,z)$, since the mathematical manipulations required herein do not require us to distinguish these two field components. Appropriate associations between $E_z(r,z)$ and $H_z(r,z)$ and the results of this section will be made as required in later sections.

From the form of $F(r,\phi,z)$ we know that there is a Fourier-Bessel transform representation (cf. [6]) for $\Phi(r,z)$, whence

$$\Phi(r,z) = \int_0^\infty \tilde{\Phi}_\nu(\alpha,z) J_\nu(k_o\alpha r)\alpha\, d\alpha \tag{2.2}$$

$$\tilde{\Phi}(\alpha,z) = k_o^2 \int_0^\infty \Phi(r,z) J_\nu(k_o\alpha r) r\, dr \tag{2.3}$$

where J_ν is a Bessel function of order ν. We shall refer to $\Phi(r,z)$ as the field and to $\tilde{\Phi}(r,z)$ as the field transform.

Substitution of (2.2) into (2.1) produces the result

$$\left\{\frac{\partial^2}{\partial z^2} + k_o^2(n'^2 - \alpha^2)\right\} \tilde{\Phi}_\nu(\alpha,z) = 0 \tag{2.4}$$

where $n' = n_1$ for $z > 0$, and $n' = n_2$ for $z < 0$.

If we consider $z = z'$, where $z'' < z' < 0$, as a plane in which point sources lie, and if we likewise require that the field should vanish for $|z| \to \infty$, then (2.4) has solutions

$$\tilde{\Phi}_\nu(\alpha,z) = A(\alpha)e^{-k_o u_1 z}, \quad z \geq 0 \tag{2.5}$$

$$\tilde{\Phi}_\nu(\alpha,z) = B_p(\alpha)e^{-k_o u_2 z} + B_n(\alpha)e^{k_o u_2 z} \quad z' \leq z \leq 0 \tag{2.6}$$

$$\tilde{\Phi}_\nu(\alpha,z) = C(\alpha)e^{k_o u_2 z}, \quad z \leq z' \tag{2.7}$$

where

$$u_1 = (\alpha^2 - n_1^2)^{1/2}, \quad \text{Re } u_1 > 0 \tag{2.8}$$

$$u_2 = (\alpha^2 - n_2^2)^{1/2}, \quad \text{Re } u_2 > 0 \tag{2.9}$$

With (2.5), (2.6), and (2.7) we have determined the field transforms except for a set of multiplicative factors dependent upon α. In the following sections we will apply source and boundary conditions to determine these factors. At that time it will be necessary to identify our field $\Phi(r,z)$ as either the electric field $E_z(r,z)$ or the magnetic field $H_z(r,z)$.

To facilitate the asymptotic analysis of Chapter 3, it is desirable to extend the range of integration in (2.2) to the negative α axis. To do this we recall that

$$J_\nu(\sigma\alpha) = \tfrac{1}{2}\{H_\nu^{(1)}(\sigma\alpha) + H_\nu^{(2)}(\sigma\alpha)\}$$

and employ the circuital relations for the Bessel functions so that (2.2) becomes

$$\phi(r,z) = \tfrac{1}{2} \int_{\infty e^{-i\pi}}^{\infty} \tilde{\phi}_\nu(\alpha,z) H_\nu^{(2)}(k_0 r\alpha)\alpha d\alpha \qquad (2.10)$$

Figure 2.1 illustrates the integration contour of $\phi(r,z)$ in the complex α-plane. The branch cuts associated with n_1 and n_2 are those which must not be crossed if we are to insure that $\mathrm{Re}\ u_1 > 0$ and $\mathrm{Re}\ u_2 > 0$. Some slight loss is assumed in both the covering medium and the substrate in order to impart a small imaginary component to both n_1 and n_2. The branch cut running along the negative real axis insures that $H_\nu^{(2)}(k_0\alpha r)$ in (2.10) is single-valued.

2.3 Evaluation of the Field Transforms

2.3.1 Equivalent Polarization Sources

The concept upon which the analysis of this section rests is that of equivalent polarization currents (cf. [7]) which can be used to convert the sourceless three medium problem into an equivalent two medium problem with sources below the dielectric interface. This approach attributes the fields existing outside the dielectric channel to the radiation from an array of polarization current sources contained within the geometrical boundaries of the channel waveguide but embedded in the substrate medium only. This circumstance is illustrated in Figure 2.2.

The justification for this procedure follows from a consideration of the differential form of Ampere's Law, i.e., the curl $\bar{H}$ relation from Maxwell's equations. In the channel region, we have

$$\nabla \times \bar{H} = i w n^2 \varepsilon_0 \bar{E} \qquad (2.11)$$

and in the substrate region the fields must satisfy

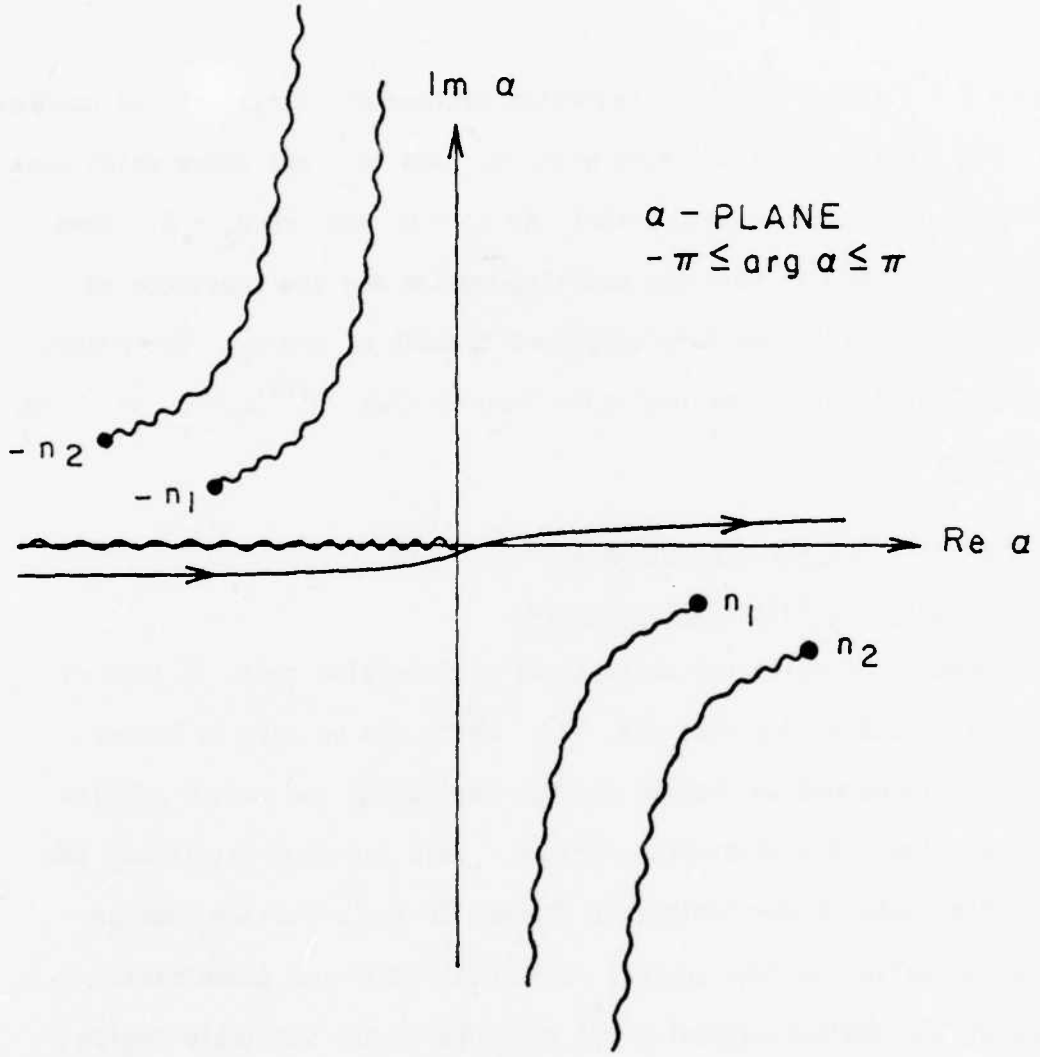

Figure 2.1 The Contour of Integration for $\Phi(r,z)$ in the Complex α-Plane

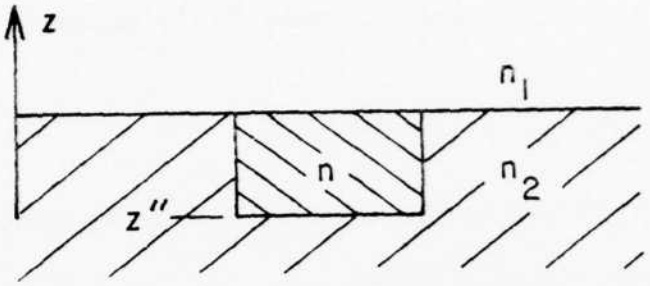

(a) THE ORIGINAL THREE MEDIUM PROBLEM WITHOUT SOURCES

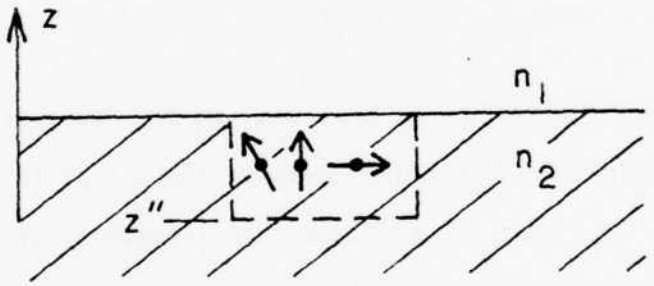

(b) THE EQUIVALENT TWO MEDIUM PROBLEM WITH POLARIZATION CURRENT SOURCES

Figure 2.2 Alternative, Equivalent Problem Representations

$$\nabla \times \bar{H} = i w n_2^2 \varepsilon_o \bar{E} \tag{2.12}$$

In (2.11) we add and subtract $j w n_2^2 \varepsilon_o \bar{E}$, then (2.11) becomes

$$\nabla \times \bar{H} = i w (n_2^2 - n^2)\, \varepsilon_o \bar{E} + i w n_2 \varepsilon_o \bar{E} \tag{2.13}$$

We now identify the first-term on the RHS of (2.13) as the equivalent polarization current density $\bar{J}_p$, thus

$$\bar{J}_p = i w (n_2^2 - n^2)\, \varepsilon_o \bar{E} \tag{2.14}$$

and (2.13) is now

$$\nabla \times \bar{H} = \bar{J}_p + i w n_2^2 \varepsilon_o \bar{E} \tag{2.15}$$

Comparison of (2.15) with (2.12) shows that we may now characterize the fields below the dielectric interface through the use of (2.15) alone, as long as we keep in mind that the equivalent polarization currents exist only within the region occupied by the channel guide. Since the only refractive index that appears explicitly in (2.15) is n_2, our problem is seen to be equivalent to that of a two-medium interface problem with sources as illustrated in Figure 2.2b.

It should be emphasized again that to solve the problem discussed herein we assume that the fields $\bar{E}_o$ and $\bar{H}_o$ in the channel guide are known, and the implication of this assumption in the present discussion is that $\bar{J}_p$ will be given explicitly as

$$\bar{J}_p = i w (n_2^2 - n^2) \varepsilon_o \bar{E}_o \tag{2.16}$$

We have thus converted information about known channel fields into a known distribution of equivalent current sources. Since $\bar{E}_o$ will in general be

capable of resolution along each of the three mutually perpendicular axes of the local coordinate system (cf. Figure 1.2) (2.16) reveals that we will in general have polarization currents directed along all three of the local coordinate axes. The remainder of this chapter is devoted to finding the field transform amplitudes associated with each unique component of the polarization currents. The total electric and magnetic fields outside the channel will ultimately be constructed via superposition of the results obtained for the special cases to be considered currently.

2.3.2 z-Directed Phased Arrays of Polarization Currents

We consider a z-directed, phased array of polarization currents located at a radius r' from the z-axis and a distance z' below the dielectric interface as illustrated in Figure 2.3. Analytically, polarization line current densities of unit amplitude along the z-direction are given by

$$\hat{J}_p = \bar{a}_z \delta(z-z')\,\delta(r-r')e^{-i\nu\phi} \tag{2.17}$$

hence reference to (2.16) gives

$$\bar{J}_p = iw(n^2-n_2^2)\varepsilon_o E_{oz}\hat{J}_p\,dr'dz' \tag{2.18}$$

To facilitate the analysis of this section we shall consider a z-directed electric type Hertzian potential of the form

$$\bar{\Pi}^e(r,\phi,z) = \bar{a}_z e^{-i\nu\phi}\int_0^\infty \tilde{\Pi}_z^e(\alpha,z)J_\nu(k_o r\alpha)\alpha d\alpha,$$

so that

$$\Pi_z^e(r,z) = \int_0^\infty \tilde{\Pi}_z^e(\alpha,z)J_\nu(k_o r\alpha)\alpha d\alpha \tag{2.19a}$$

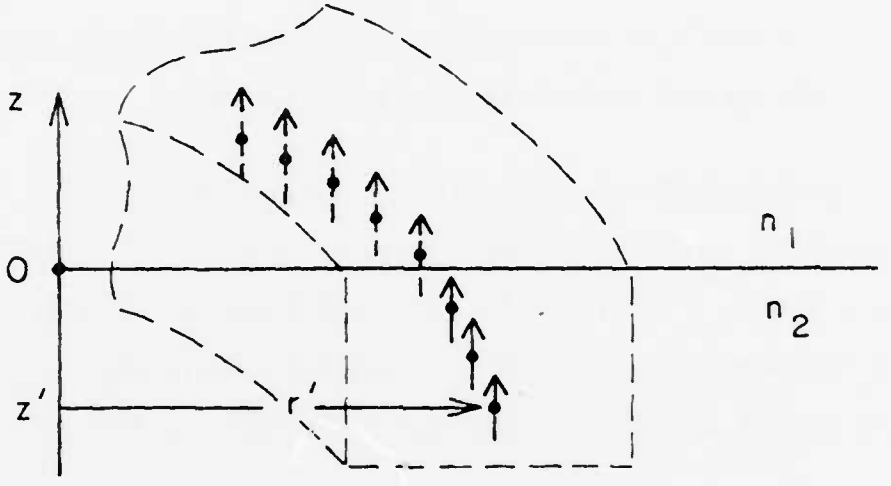

Figure 2.3 A z-Directed Phased Array of Polarization Currents

and

$$\tilde{\Pi}^e_z(\alpha,z) = k_o^2 \int_0^\infty \Pi^e_z(r,z) J_\nu(k_o r\alpha) r dr \tag{2.19b}$$

In this section we will be dealing with the cartesian component of the electric field only, because $H_z \equiv 0$ for a z-directed Hertzian potential.

The Hertzian potential satisfies the inhomogeneous wave equation (cf. [8])

$$(\nabla^2 + k_{1,2}^2)\vec{\Pi}^e = \frac{-\hat{J}_p}{i w \varepsilon_o n_2^2} \tag{2.20}$$

where $k_{1,2} = n_{1,2} k_o$, thus using (2.17) in (2.20)

$$(\nabla^2 + k_{1,2}^2)\Pi^e_z(r,z) = -\left(\frac{1}{i w \varepsilon_o n_2^2}\right) \delta(z-z') \delta(r-r') \tag{2.21}$$

Substitution of (2.19a) into (2.21) and use of the Fourier-Bessel representation of $\delta(r-r')$ yields

$$\left\{\frac{\partial^2}{\partial z^2} - k_0^2 u_{1,2}^2\right\} \tilde{\Pi}^e_z(\alpha,z) = \left[\frac{-k_o^2 r'}{i w \varepsilon_o n_2^2}\right] J_\nu(k_o r'\alpha) \delta(z-z') \tag{2.22}$$

where, as in (2.8) and (2.9), $u_{1,2} = (\alpha^2 - n_{1,2}^2)^{\frac{1}{2}}$.

Following the same line of reasoning as in Section 2.2, we have the following solutions for $\tilde{\Pi}^e_z(\alpha,z)$ from (2.22):

$$\tilde{\Pi}^e_z(\alpha,z) = A(\alpha) e^{-k_o u_1 z}, \quad z \geq 0 \tag{2.23a}$$

$$\tilde{\Pi}^e_z(\alpha,z) = B_p(\alpha) e^{-k_o u_2 z} + B_n(\alpha) e^{k_o u_2 z}, \quad z' \leq z \leq 0 \tag{2.23b}$$

$$\tilde{\Pi}^e_z(\alpha,z) = C(\alpha) e^{-k_o u_2 z}, \quad z \leq z' \tag{2.23c}$$

We solve for the transform coefficients $A(\alpha)$, $B_p(\alpha)$, $B_n(\alpha)$, and $C(\alpha)$ via application of source conditions at $z = z'$ (two equations) and boundary conditions at $z = 0$ (two equations); this yields

$$A(\alpha) = \frac{u_2 n_{2r'}^2}{u_1 n_2^2 + u_2 n_1^2} \left\{ \frac{k_o J_\nu(k_o r'\alpha)}{i u_2 w \varepsilon_o n_2^2} \right\} e^{k_o u_2 z'} \tag{2.24a}$$

$$B_p(\alpha) = \frac{k_o J_\nu(k_o r'\alpha) r'}{i 2 u_2 w \varepsilon_o n_2^2} e^{k_o u_2 z'} \tag{2.24b}$$

$$B_n(\alpha) = \frac{k_o J_\nu(k_o r'\alpha) r'}{i 2 u_2 w \varepsilon_o n_2^2} \left\{ \frac{u_2 n_1^2 - u_1 n_2^2}{u_2 n_1^2 + n_1 u_2^2} \right\} e^{k_o u_2 z'} \tag{2.24c}$$

$$C(\alpha) = \frac{k_o J_\nu(k_o r'\alpha) r'}{i 2 u_2 w \varepsilon_o n_2^2} \left\{ e^{-k_o u_2 z'} + \frac{u_2 n_1^2 - u_1 n_2^2}{u_2 n_1^2 + u_1 n_2^2} e^{k_o u_2 z'} \right\} \tag{2.24d}$$

We can now use (2.24a) through (2.24d) in (2.23a) through (2.23c) in order to produce the following expressions for the potential transforms

$$\tilde{\Pi}_z^e(\alpha, z) = \frac{k_o J_\nu(k_o r'\alpha) r'}{i 2 u_2 w \varepsilon_o n_2^2} \left\{ \frac{2 u_2 n_2^2}{u_1 n_2^2 + u_2 n_1^2} \right\} e^{k_o (u_2 z' - u_1 z)}, \quad z \geq 0 \tag{2.25a}$$

$$\tilde{\Pi}_z^e(\alpha, z) = \frac{k_o J_\nu(k_o r'\alpha) r'}{i 2 u_2 w \varepsilon_o n_2^2} \left\{ e^{-k_o u_2 |z - z'|} + \frac{u_2 n_1^2 - u_1 n_2^2}{u_2 n_1^2 + u_1 n_2^2} e^{k_o u_2 (z + z')} \right\}, \quad z \leq 0 \tag{2.25b}$$

Substitution of (2.25a) and (2.25b) into (2.19a) produces the desired integral representations for the Hertzian potential in the covering region ($z \geq 0$) and the substrate region ($z \leq 0$):

$$\Pi_z^e(r,z) = -i\zeta_o r' \int_0^\infty \left(\frac{u_2}{u_1 n_2^2 + u_2 n_1^2}\right) J_\nu(k_o r'\alpha) J_\nu(k_o r\alpha) e^{k_o(u_2 z' - u_1 z)} \frac{\alpha d\alpha}{u_2}$$

$$z \geq 0 \qquad (2.26a)$$

$$\Pi_z^e(r,z) = \frac{-i\zeta_o r'}{2n_2^2} \int_0^\infty \left\{ e^{-k_o u_2 |z-z'|} + \left[\frac{u_2 n_1^2 - u_1 n_2^2}{u_2 n_1^2 + u_1 n_2^2}\right] e^{k_o u_2 (z+z')} \right\}$$

$$J_\nu(k_o r'\alpha) J_\nu(k_o r\alpha) \frac{\alpha d\alpha}{u_2} \quad , \quad z \leq 0 \qquad (2.26b)$$

where we have used $\frac{wu_o}{k_o} = \zeta_o$, the intrinsic wave impedance of free-space.

Proceeding as was done to extend the range of integration of (2.2) to yield (2.10), we may extend the range of integration in (2.26a) and (2.26b) to give

$$\Pi_z^e(r,z) = \frac{-i\zeta_o r'}{2} \int_{\infty e^{-i\pi}}^\infty \left[\frac{u_2}{u_1 n_2^2 + u_2 n_1^2}\right] H_\nu^{(2)}(k_o \alpha r) J_\nu(k_o r'\alpha) e^{k_o(u_2 z' - u_1 z)}$$

$$\frac{\alpha d\alpha}{u_2} \quad , \quad z \geq 0 \qquad (2.27a)$$

$$\Pi_z^e(r,z) = \frac{-i\zeta_o r'}{4n_2^2} \int_{\infty e^{-i\pi}}^\infty \left\{ e^{-k_o u_2 |z-z'|} + \frac{u_2 n_1^2 - u_1 n_2^2}{u_2 n_1^2 + u_1 n_2^2} e^{k_o u_2 (z+z')} \right\}$$

$$H_\nu^{(2)}(k_o r\alpha) J_\nu(k_o r'\alpha) \frac{\alpha d\alpha}{u_2} \quad , \quad z \leq 0 \qquad (2.27b)$$

2.3.3 r-Directed Phased Arrays of Polarization Currents

We consider an r-directed phased array of polarization currents located at a radius r' from the z-axis and at a distance z' below the dielectric interface as illustrated in Figure 2.4. Figure 2.4b is a cross-sectional view while Figure 2.4a is a view as seen from the covering medium looking down on the z-axis.

Analytically, the polarization current sources of unit amplitude are given by

$$\hat{J}_p = \bar{a}_r \delta(z-z')\,\delta(r-r')e^{-iv\phi} \tag{2.28}$$

hence

$$\bar{J}_p = iw(n^2-n_2^2)\varepsilon_o E_{or}\hat{J}_p dr'dz' \tag{2.29}$$

The approach taken in this section is to consider directly the cartesian components of the electric and magnetic fields. We have seen in Section 2.2 that E_z and H_z satisfy the Helmholtz equation in source-free regions and thus that their associated field (Fourier-Bessel) transforms satisfy equations (2.5), (2.6), and (2.7). In light of the results in Section 2.3.2, we will hypothesize from the start the following forms for the field transforms

$$\tilde{\phi}_r^{e,m}(\alpha,z) = A_r^{e,m}(\alpha)e^{-k_o(u_1 z-u_2 z')}, \quad z \geq 0 \tag{2.30a}$$

$$\tilde{\phi}_r^{e,m}(\alpha,z) = B_{pr}^{e,m}(\alpha)e^{k_o u_2(z+z')} + B_{nr}^{e,m}(\alpha)e^{-k_o u_2(z-z')}, \quad z' \leq z \leq 0 \tag{2.30b}$$

$$\tilde{\phi}_r^{e,m}(\alpha,z) = C_r^{e,m}(\alpha)e^{k_o u_2 z}, \quad z \leq z' \tag{2.30c}$$

where we will make the associations $\tilde{\phi}_r^e \triangleq \tilde{E}_z$ and $\tilde{\phi}_r^m \triangleq \tilde{H}_z$, and the subscript

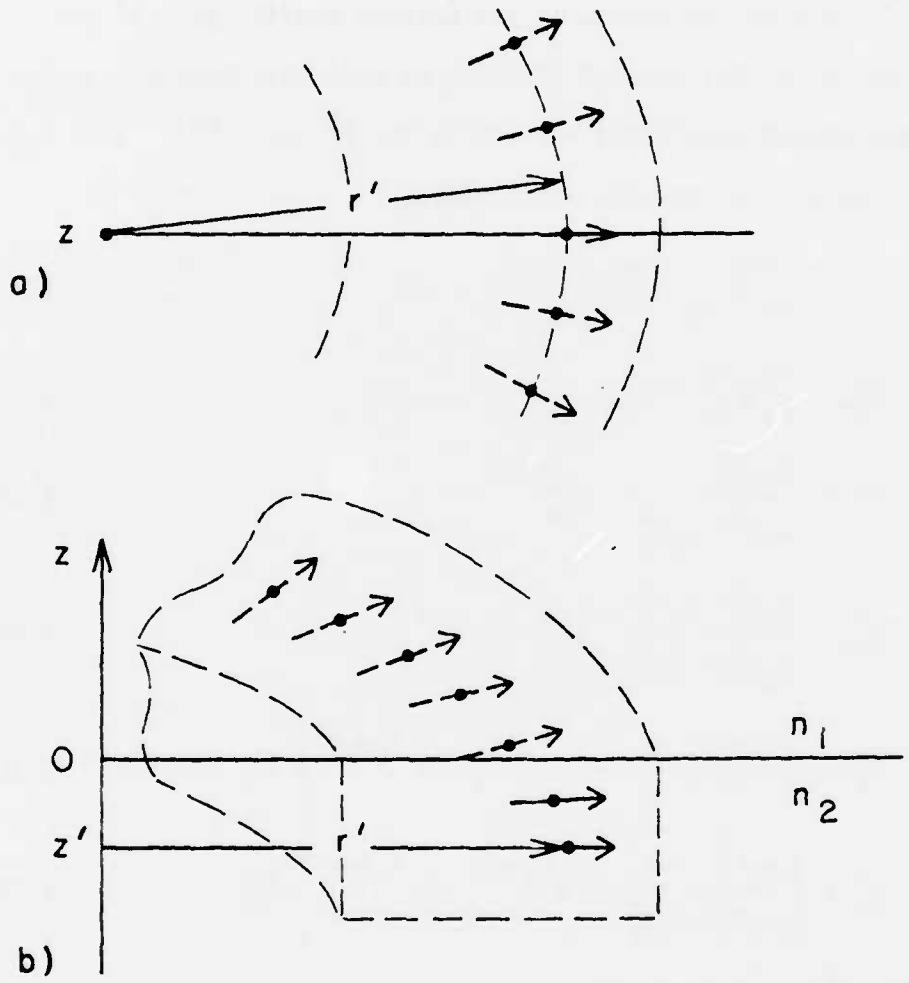

Figure 2.4 An r-Directed Phased Array of Polarization Currents

r indicates that these are field transforms associated with r-directed polarization currents.

In order to compute the eight, as yet unknown coefficients of the field transforms in (2.30a) through (2.30c), we must determine and apply the boundary and source conditions applicable to $\tilde{\Phi}^e_r$ and $\tilde{\Phi}^m_r$. This process is presented in detail in Appendix A and yields:

$$A^m_r = \frac{2u_2}{u_1 + u_2} B^m_{pr} \tag{2.31a}$$

$$B^m_{nr} = \frac{u_2 - u_1}{u_2 + u_1} B^m_{pr} \tag{2.31b}$$

$$A^e_r = \frac{2u_2 n_2^2}{u_2 n_1^2 + u_1 n_2^2} B^e_p \tag{2.31c}$$

$$B^e_{nr} = \frac{u_2 n_1^2 - u_1 n_2^2}{u_2 n_1^2 + u_1 n_2^2} B^e_p \tag{2.31d}$$

$$D^m_r = \left\{ \frac{u_2 - u_1}{u_1 + u_2} e^{k_o u_2 z'} - e^{-k_o u_2 z'} \right\} B^m_{pr} \tag{2.31e}$$

$$D^e_r = \left\{ \frac{u_2 n_1^2 - u_1 n_2^2}{u_2 n_1^2 + u_1 n_2^2} e^{k_o u_2 z'} - e^{-k_o u_2 z'} \right\} B^e_{pr} \tag{2.31f}$$

where B^m_{pr} and B^e_{pr} are given by

$$B^m_{pr} = \frac{i\gamma R_o k_o^2}{2u_2} J_\nu(k_o \alpha r') \tag{2.32a}$$

$$B^e_{pr} = \frac{\alpha r' \zeta_o k_o^2}{i2n_2^2} J'_\nu(k_o \alpha r') \tag{2.32b}$$

Substitution of (2.31a) through (2.31f) into (2.30a) through (2.30c) yields the following forms for the field transforms:

$$\tilde{\Phi}^{e}_{r}(\alpha,z) = B^{e}_{pr}\ \frac{2u_2n_2^2}{u_2n_1^2 + u_1n_2^2}\ e^{-k_o(u_1z-u_2z')}, \quad z \geq 0 \tag{2.33a}$$

$$\tilde{\Phi}^{e}_{r}(\alpha,z) = B^{e}_{pr}\left\{\frac{u_2n_1^2 - u_1n_2^2}{u_2n_1^2 + u_1n_2^2}\ e^{k_ou_2(z+z')} + \mathrm{sgn}[(z-z')]e^{-k_ou_2|z-z'|}\right\} \quad z \leq 0 \tag{2.33b}$$

and

$$\tilde{\Phi}^{m}_{r}(\alpha,z) = B^{m}_{pr}\ \frac{2u_2}{u_1+u_2}\ e^{-k_o(u_1z-u_2z')}, \quad z \geq 0 \tag{2.34a}$$

$$\tilde{\Phi}^{m}_{r}(\alpha,z) = B^{m}_{pr}\left\{\frac{u_2 - u_1}{u_2 + u_1}\ e^{k_ou_2(z+z')} + e^{-k_ou_2|z-z'|}\right\}, \quad z \leq 0 \tag{2.34b}$$

where sgn[(z-z')] in (2.33b) is the numerical sign of (z-z').

With the field transforms thus specified, we may employ (2.10) directly in order to generate the desired integral representations for the cartesian components of the electric and magnetic fields in the covering and substrate regions, hence

$$\Phi^{e}_{r}(r,z) = \frac{k_o^2\zeta_o r'}{i4n_2^2}\int_{\infty e^{-i\pi}}^{\infty} J'_\nu(k_o\alpha r')H^{(2)}_\nu(k_o\alpha r)\left[\frac{2u_2n_2^2}{u_2n_1^2 + u_1n_2^2}\right]e^{-k_o(u_1z-u_2z')}\ \alpha^2 d\alpha, \quad z \geq 0 \tag{2.35a}$$

$$\tilde{\Phi}^{e}_{r}(r,z) = \frac{k_o\zeta_o r'}{i4n_2^2}\int_{\infty e^{-i\pi}}^{\infty} J'_\nu(k_o\alpha r')H^{(2)}_\nu(k_o\alpha r)\left\{\frac{u_2n_1^2 - u_1n_2^2}{u_2n_1^2 + u_1n_2^2}\ e^{k_ou_2(z+z')} + \mathrm{sgn}[(z-z')]e^{-k_ou_2|z-z'|}\right\}\alpha^2 d\alpha \quad z \geq 0 \tag{2.35b}$$

$$\Phi^{m}_{r}(r,z) = \frac{i\gamma R_o k_o^2}{4} \int_{\infty e^{-i\pi}}^{\infty} J_\nu(k_o r') H (k_o \alpha r) \frac{2u_2}{u_1+u_2} e^{-k_o u_2 (z-z')} \frac{\alpha d\alpha}{u_2}, \quad z \geq 0 \tag{2.36a}$$

$$\Phi^{m}_{r}(r,z) = \frac{i\gamma R_o k_o^2}{2} \int_{\infty e^{-i\pi}}^{\infty} J_\nu(k_o \alpha r') H^{(2)}(k_o \alpha r) \left\{ \frac{u_2-u_1}{u_2+u_1} e^{k_o u_2 (z+z')} + e^{-k_o u_2 |z-z'|} \right\} \frac{\alpha d\alpha}{u_2}, \quad z \leq 0 \tag{2.36b}$$

where (2.35a), (2.35b), (2.36a), and (2.36b) are integrated along the contour shown in Figure 2.1.

Finally, with reference to (2.27a) and (2.27b), we see that (2.35a) and (2.35b) can be related to $\Pi^{e}_{z}(r,z)$ by

$$\Phi^{e}_{r}(r,z) = r' \frac{\partial^2}{\partial r' \partial z'} \frac{1}{r'} \Pi^{e}_{z}(r,z) \tag{2.37}$$

2.3.4 ϕ-Directed Phased Arrays of Polarization Current

As per Section 2.3.3, we consider the cartesian components $\Phi^{e}_{\phi} \triangleq E_z$ and $\Phi^{m}_{\phi} \triangleq H_z$ of the electric and magnetic fields in the covering and substrate media. The procedure for finding integral representations of these cartesian field components is very similar to that followed above. Indeed, the only formal difference between the case currently under consideration and that of the r-directed polarization currents is that the unit vector in the representation of the polarization current densities changes from $\bar{a}_r$ to $\bar{a}_\phi$, with the result that (A.3c) and (A.3d) [cf. Appendix A] are replaced, respectively, by

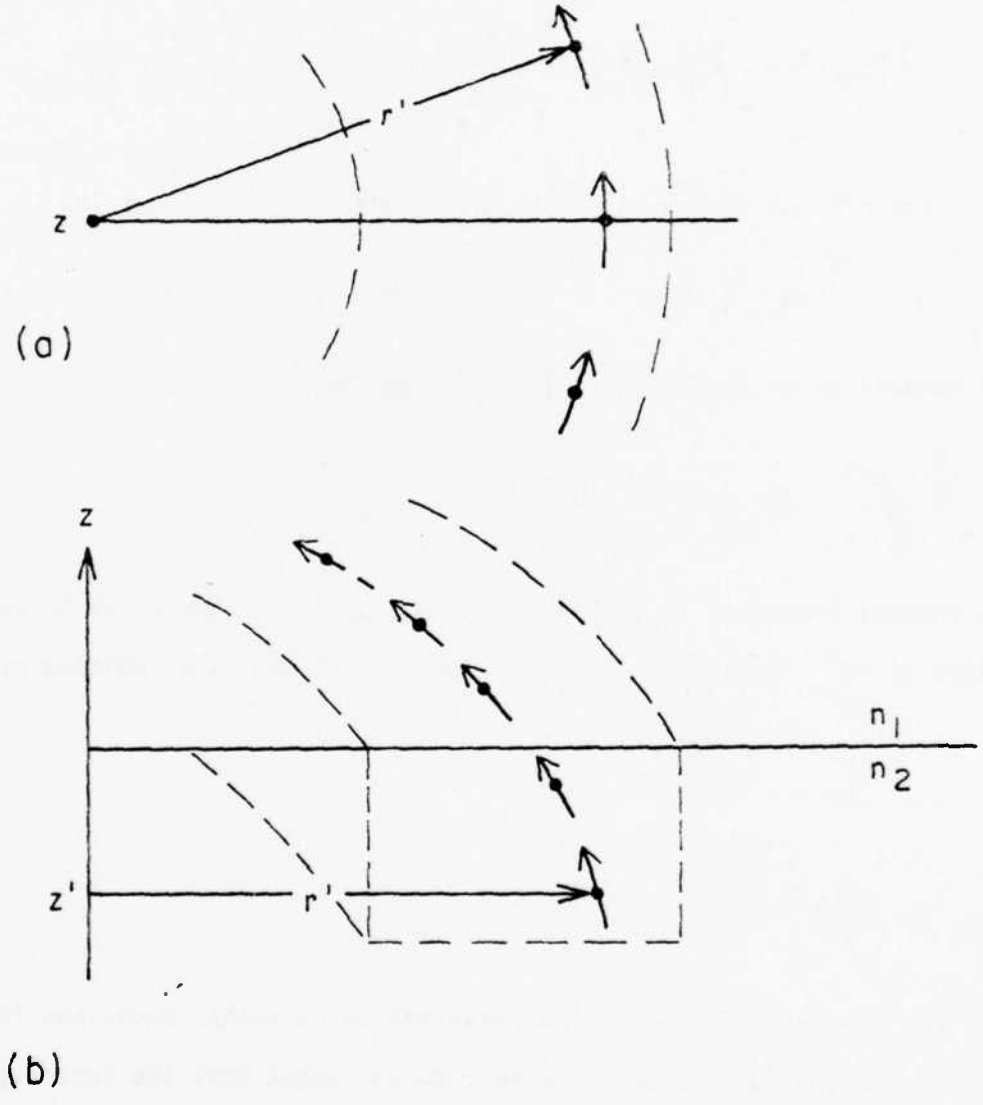

Figure 2.6 A ϕ-Directed Pgased Array of Polarization Currents

$$\frac{\partial}{\partial z}\tilde{\Phi}^m_\phi(\alpha,z)\Big|_{z=z'+} - \frac{\partial}{\partial z}\tilde{\Phi}^m_\phi(\alpha,z)\Big|_{z=z'-} = k_o^3\, r' J'_\nu\,(k_o\alpha r') \tag{2.38a}$$

$$\tilde{\Phi}^e_\phi(\alpha,z'+) - \tilde{\Phi}^e_\phi(\alpha,z'-) = \frac{\nu k_o^2}{w\epsilon_o n_2^2}\, J_\nu(k_o\alpha r') \tag{2.38b}$$

Comparing (2.38a) with (A.3c) (recalling $\nu = \gamma k_o R_o$) we see

$$-i\gamma R_o k_o^3 J_\nu(k_o\alpha r') \to k_o^3 \alpha r' J'_\nu(k_o\alpha r') \tag{2.39}$$

and comparison of (2.38b) with (A.3d) shows that

$$\frac{k_o^2\,\zeta_o \alpha r'}{in_2^2}\, J'_\nu(k_o\alpha r') \to \gamma \frac{R_o k_o^2 \zeta_o}{n_2^2}\, J_\nu(k_o\alpha r') \tag{2.40}$$

The changes indicated in (2.39) and (2.40) manifest themselves in the values of $B^m_{p\phi}$ and $B^e_{p\phi}$. Thus, (2.32a) and (2.32b) are replaced by

$$B^m_{p\phi} = \frac{-k_o^2 \alpha r'}{2u_2}\, J'_\nu(k_o\alpha r') \tag{2.41a}$$

$$B^e_{p\phi} = \frac{\gamma R_o k_o^2 \zeta_o}{2n_2^2}\, J_\nu(k_o\alpha r') \tag{2.41b}$$

For the case of ϕ-directed polarization currents, equations (2.33a), (2.33b) and (2.34a), (2.34b) are reproduced except that the subscript r is replaced by the subscript ϕ. Using (2.33a) through (2.34b) modified for ϕ-directed currents in (2.10) we have

$$\Phi_{\phi}^{e}(r,z) = \frac{\gamma R_o \zeta_o k_o^2}{4n_2^2} \int_{\infty e^{-i\pi}}^{\infty} J_\nu(k_o\alpha r')H_\nu^{(2)}(k_o\alpha r)$$

$$\frac{2u_2 n_2^2}{u_2 n_1^2 + u_1 n_2^2} \; e^{-k_o(u_1 z - u_2 z')} \; \alpha d\alpha \,, \qquad z \geq 0 \tag{2.42a}$$

$$\Phi_{\phi}^{e}(r,z) = \frac{\gamma R_o \zeta_o k_o^2}{4n_2^2} \int_{\infty e^{-i\pi}}^{\infty} J_\nu(k_o\alpha r')H_\nu^{(2)}(k_o\alpha r)$$

$$\left\{ \frac{u_2 n_1^2 - u_1 n_2^2}{u_2 n_1^2 + u_1 n_2^2} \; e^{k_o u_2 (z+z')} + \mathrm{sgn}[(z-z')] e^{-k_o u_2 |z-z'|} \right\} \alpha d\alpha \,,$$

$$z \leq 0 \tag{2.42b}$$

$$\Phi_{\phi}^{m}(r,z) = \frac{-k_o^2 r'}{4} \int_{\infty e^{-i\pi}}^{\infty} J_\nu'(k_o\alpha r')H_\nu^{(2)}(k_o\alpha r)$$

$$\frac{2u_2}{u_1+u_2} \; e^{-k_o u_2 (z-z')} \; \frac{\alpha^2 d\alpha}{u_2} \qquad z \geq 0 \tag{2.42c}$$

$$\Phi_{\phi}^{m}(r,z) = \frac{-k_o^2 r'}{4} \int_{\infty e^{-i\pi}}^{\infty} J'(k_o\alpha r')H_\nu^{(2)}(k_o\alpha r)$$

$$\left\{ \frac{u_2 - u_1}{u_2 + u_1} \; e^{k_o u_2 (z+z')} + e^{-k_o u_2 |z-z'|} \right\} \; \frac{\alpha^2 d\alpha}{u_2} \qquad z \leq 0 \tag{2.42d}$$

Upon comparison of (2.42a) and (2.42c) with (2.27a) and (2.27b), respectively, we see

$$\Phi_{\phi}^{e}(r,z) = \frac{i\gamma R_o k_o}{r'} \; \frac{\partial}{\partial z'} \; \Pi_z^e(r,z) \tag{2.43}$$

Finally, comparison of (2.42c) and (2.42d) with (2.36a) and (2.36b), respectively, yields

$$\Phi_{\phi}^{m}(r,z) = \frac{-r'}{i\gamma R_o k_o} \; \frac{\partial}{\partial r'} \; \Phi_r^m(r,z) \tag{2.44}$$

2.3.5 The Ancillary Potential Integrals V_e, V_m

In terms of the Hertzian potential Π_z^e of Section 2.3.2, we can write the associated cartesian component of the electric field ϕ_z^e as

$$\phi_z^e(r,z) = \left(\frac{\partial^2}{\partial z^2} + k_{1,2}^2\right)\Pi_z^e \tag{2.45}$$

Now, considering (2.27a) and (2.27b) we define the scalar, electric, ancillary potential V_e by

$$V_e(r,z) = \left(\frac{-i\zeta_o}{4n_2^2}\right)\int_{\infty e^{-i\pi}}^{\infty} J_\nu(k_o r'\alpha)H_\nu^{(2)}(k_o r\alpha)$$

$$\frac{2u_2 n_2^2}{u_1 n_2^2 + u_2 n_1^2}\, e^{k_o(u_2 z' - u_1 z)}\, \frac{\alpha d\alpha}{u_2}\,, \qquad z \geq 0 \tag{2.46a}$$

$$V_e(r,z) = \frac{-i\zeta_o}{4n_2^2}\int_{\infty e^{-i\pi}}^{\infty} J_\nu(k_o r'\alpha)H_\nu^{(2)}(k_o r\alpha)$$

$$\left\{\frac{u_2 n_1^2 - u_1 n_2^2}{u_2 n_1^2 + u_1 n_2^2}\, e^{k_o u_2 (z+z')} + e^{-k_o u_2 |z-z'|}\right\}\frac{\alpha d\alpha}{u_2}\,, \qquad z \leq 0 \tag{2.46b}$$

Having thus defined V_e, we see that

$$\phi_z^e(r,z) = r'\left\{\frac{\partial^2}{\partial z^2} + k_{1,2}^2\right\}V_e(r,z) \tag{2.47a}$$

In a like manner, considering (2.46a) and (2.46b) along with (2.35a) and (2.35b), we have

$$\phi_r^e(r,z) = r'\,\frac{\partial^2}{\partial r'\partial z'}\,V_e(r,z) \tag{2.47b}$$

Consider now the definition of the scalar, magnetic, ancillary potential V_m given as

$$V_m(r,z) = \left(\frac{k_o}{4}\right) \int_{\infty e^{-i\pi}}^{\infty} J_\nu(k_o r'\alpha) H_\nu^{(2)}(k_o r\alpha)$$

$$\frac{2u_2}{u_1+u_2} e^{-k_o(u_1 z - u_2 z')} \frac{\alpha d\alpha}{u_2}, \qquad z \geq 0 \tag{2.48a}$$

$$V_m(r,z) = \left(\frac{k_o}{4}\right) \int_{\infty e^{-i\pi}}^{\infty} J_\nu(k_o r') H_\nu^{(2)}(k_o r)$$

$$\left\{ \frac{u_2-u_1}{u_2+u_1} e^{k_o u_2(z+z')} + e^{-k_o u_2 |z-z'|} \right\} \frac{\alpha d\alpha}{u_2}, \qquad z \leq 0 \tag{2.48b}$$

Comparison of (2.48a) and (2.48b) with (2.36a) and (2.36b) gives

$$\Phi_r^m(r,z) = (i\gamma R_o k_o) V_m \tag{2.48c}$$

and a similar comparison of (2.48a) and (2.48b) with (2.42c) and (2.42d) yields

$$\Phi_\phi^m(r,z) = -r' \frac{\partial}{\partial r'} V_m \tag{2.48d}$$

We can conveniently summarize the representation of the total cartesian field components Φ^e and Φ^m due to polarization currents in the channel region in terms of the potentials V_e and V_m, i.e., since

$$\Phi^e = \Phi_z^e + \Phi_r^e + \Phi_\phi^e \quad \text{and} \quad \Phi^m = \Phi_r^m + \Phi_\phi^m ,$$

we can write

$$\begin{bmatrix} \Phi^e(r,z) \\ \Phi^m(r,z) \end{bmatrix} = i\omega\varepsilon_o(n^2-n_2^2) \int_{\substack{\text{Guide} \\ \text{Cross} \\ \text{Section}}} dS' \begin{bmatrix} r' \frac{\partial^2 V_e}{\partial r' \partial z'} & \left[i\gamma R_o k_o \frac{\partial V_e}{\partial z'} \right] & r' \left\{ \frac{\partial^2}{\partial z^2} + k_{1,2}^2 \right\} V_e \\ i\gamma R_o k_o V_m & \left\{ -r' \frac{\partial}{\partial r'} V_m \right\} & 0 \end{bmatrix} \begin{bmatrix} E_{or} \\ E_{o\phi} \\ E_{oz} \end{bmatrix} \tag{2.49}$$

CHAPTER 3

ASYMPTOTIC EVALUATION OF THE ANCILLARY POTENTIAL V_e

3.1 Introduction

The developments in Chapter 2 have led to a representation of the Cartesian field components exterior to the curved channel waveguide in terms of the fields of the straight channel waveguide and the ancillary electric and magnetic potentials V_e and V_m, respectively. In this chapter we will concentrate upon determining an analytical expression for V_e that is more useful in practical applications than is the formal representation in equations (2.46a), (2.46b). The ancillary potential V_m will be discussed only to a limited extent since the analytical procedure employed to simplify V_e can be applied without modification to V_m.

The analytical approach to finding a more useful representation for V_e and V_m begins with application of the Debye expansions for Bessel and Hankel functions of large order and argument to the integrands of (2.46a), (2.46b) and (2.48a), (2.48b). Once accomplished, this step is seen to facilitate an asymptotic analysis of the modified integrals. In particular, a steepest descent evaluation is pursued for V_e which yields a first order representation when $k_o R_o >> 1$.

In Chapter 4, the asymptotic expression derived for V_e is used to compute the attenuation constant due to continuous radiation loss from a bent rectangular waveguide after assuming a specific form for the straight guide modes.

3.2 Modification of the Integral Representations of V_e, V_m

3.2.1 Changing the Contour of Integration

As we have noted previously, the contour over which the integral representations of V_e and V_m are integrated is that illustrated in Figure 2.1. We now consider the closed contour Γ_c shown in Figure 3.1 which is composed of the contour γ_o which lies along the Re α axis as well as the contours γ_1, γ_2, γ_{R_1}, γ_{R_2}, γ_{R_3}. The contours γ_1 and γ_2 lie along the branch cuts associated with n_1 and n_2, respectively, and contours γ_{R_1}, γ_{R_2}, and γ_{R_3} lie on the radius of a semi-circle of radius R. We will eventually consider Γ_c as $R \to \infty$, whereupon γ_o will coincide with our original contour of integration for V_e and V_m. For the moment, however consider the integrals

$$I_G = \oint_{\Gamma_c} F(\alpha)\, e^{k_o(u_2 z' - u_1 z)}\, d\alpha\,, \qquad z \geq 0 \tag{3.1a}$$

$$I_L = \oint_{\Gamma_c} \left\{ G(\alpha) e^{k_o u_2 (z+z')} + H(\alpha) e^{-k_o u_2 |z-z'|} \right\} d\alpha\,, \qquad z \leq 0 \tag{3.1b}$$

where $F(\alpha)$, $G(\alpha)$, and $H(\alpha)$ are analytic everywhere within and on Γ_c and tend uniformly to zero as $R \to \infty$. Since there are no singularities of the integrand contained within Γ_c, the residue theorem assures that $I_G = I_L = 0$, so (3.1a) and (3.1b) give, respectively,

$$\int_{\gamma_o} (F) = -\int_{\gamma_1} (F) - \int_{\gamma_2} (F) - \int_{\gamma_{R_1}+\gamma_{R_2}+\gamma_{R_3}} (F) \tag{3.2a}$$

$$\int_{\gamma_o} (G,H) = -\int_{\gamma_1} (G,H) - \int_{\gamma_2} (G,H) - \int_{\gamma_{R_1}+\gamma_{R_2}+\gamma_{R_3}} (G,H) \tag{3.2b}$$

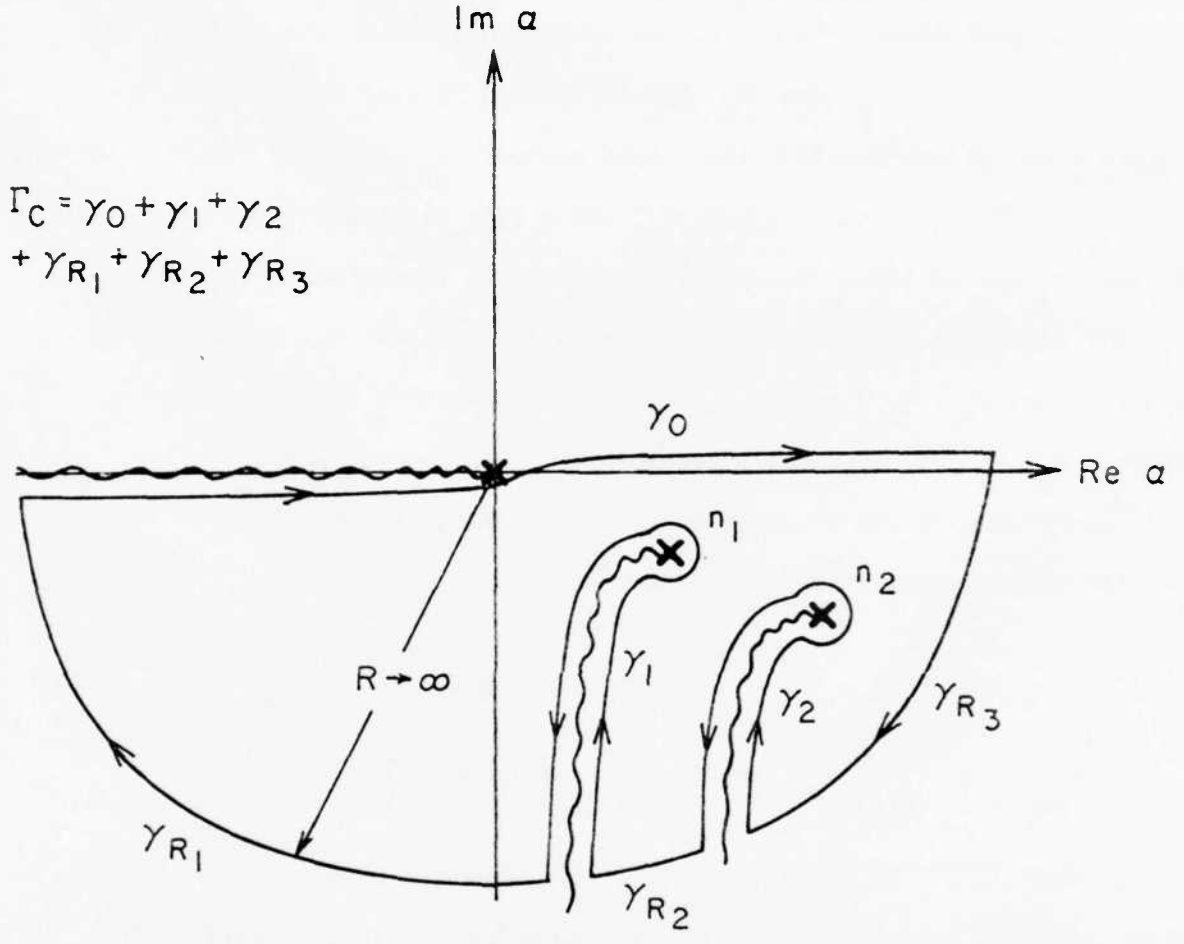

Figure 3.1 The Contour Γ_c

where we have symbolized the integrand of (3.1a) by (F) and the integrand of (3.1b) by (G,H).

If now we let $R \to \infty$, we may invoke Jordan's lemma to justify the claim that both $\int_{\gamma_{R_1}+\gamma_{R_2}+\gamma_{R_3}} (F)$ and $\int_{\gamma_{R_1}+\gamma_{R_2}+\gamma_{R_3}} (G,H)$ vanish (recall $z' < 0$).

Also, the uniform tendency toward zero of $F(\alpha)$, $G(\alpha)$, and $H(\alpha)$ together with the exponential factors in (F) and (G,H) assure the convergence of the remaining integrals, whence (3.2a) and (3.2b) become

$$\int_{\infty e^{-i\pi}}^{\infty} (F) = -\int_{\gamma_1} (F) - \int_{\gamma_2} (F) \tag{3.3a}$$

$$\int_{\infty e^{-i\pi}}^{\infty} (G,H) = -\int_{\gamma_1} (G,H) - \int_{\gamma_2} (G,H) \tag{3.3b}$$

where γ_1 and γ_2 are now contours which "wrap-around" the full extent of their associated branch cuts.

Notice that both V_e and V_m take the form of (3.3a) for $z \geq 0$, and that both V_e and V_m take the form of (3.3b) for $z \leq 0$. Thus, we can now transfer our attention from an integration of the ancillary potentials V_e and V_m along the $\mathrm{Re}\,\alpha$ axis to a pair of integrals which, in each case, follow the branch cuts of u_1 and u_2 in the lower half of the α-plane.

3.2.2 Application of the Debye Expansions

Our objective in this section is to find an asymptotic representation for the product $J_\nu(k_o r'\alpha)H_\nu^{(2)}(k_o r\alpha)$ which appears in the integrands

of the integral representations of V_e and V_m. Since we are interested in geometries for which $k_o R_o >> 1$, and since $\nu = \gamma k_o R_o$, we are certainly dealing with Bessel and Hankel functions of large order. Likewise, since we are interested in fields just beyond the outer radius of the channel guide, both r' and r are on the order of R_o; so, for α of sufficiently large modulus, the Bessel and Hankel functions we encounter are of large argument as well. The requirement that α be of sufficient modulus means that there is a region about the origin of the α-plane of radius $O(\frac{1}{k_o R_o})$ within which we cannot allow our integration contour to pass. This presents no significant difficulty since we are free to deform the contours γ_1 and γ_2 onto the improper Riemann sheet (if necessary) for a finite distance and hence to circumvent the forbidden region, whereupon we re-enter the proper sheet and continue integrating along the branch cuts. We will not consider this subtlety in greater depth since we will ultimately prosecute a saddle point evaluation of our integrals for which the saddle point is well removed from regions where the large argument assumption is invalid.

The Debye asymptotic expansions for large order and argument may be written in the form (cf.[5], [9])

$$(2\pi\nu)^{\frac{1}{2}} J_\nu(\nu z) \sim (1 - z^2)^{-\frac{1}{4}} e^{-\nu f(z)} \tag{3.4a}$$

$$(2\pi\nu)^{\frac{1}{2}} Y_\nu(\nu z) \sim -2(1-z^2)^{-\frac{1}{4}} e^{\nu f(z)} \tag{3.4b}$$

where $0 < \mathrm{Re}\, z < 1$, and

$$f(z) = \tanh^{-1}(1 - z^2)^{\frac{1}{2}} - (1-z^2)^{\frac{1}{2}} \tag{3.4c}$$

and where Y_ν is the Neumann function of order ν.

Since $H_\nu^{(2)} = J_\nu - iY_\nu$, (3.4a) and (3.4b) give

$$H_\nu^{(2)}(\nu z) \sim \frac{i2(1-z^2)^{-\frac{1}{4}}}{(2\pi\nu)^{\frac{1}{2}}} \left\{ e^{\nu f(z)} - \frac{i}{2} e^{-\nu f(z)} \right\} \tag{3.5}$$

If we let $\nu z = k_o \alpha (R_o + y)$, then

$$z = \frac{\alpha}{\gamma}\left(1 + \frac{y}{R_o}\right) \tag{3.6}$$

and

$$z_o \triangleq z\Big|_{y=0} = \frac{\alpha}{\gamma} \tag{3.7}$$

Recall that y is the radial coordinate of the local coordinate system situated at the center of the channel guide (cf. Figure 1.2). In an integrated optics environment we will have $n > \gamma > n_2$, thus inspection of the contour γ_2 reveals that $\mathrm{Re}(\frac{\alpha}{\gamma}) < 1$ for all α on γ_2.

A Taylor series expansion of (3.4c) in powers of y about z_o as given in (3.7) yields the result

$$\nu f(z) \approx k_o R_o \gamma f(\tfrac{\alpha}{\gamma}) - y k_o \gamma \left(1 - \frac{\alpha^2}{\gamma^2}\right)^{\frac{1}{2}} \tag{3.8}$$

Using (3.8) in (3.5) gives

$$H_\nu^{(2)}(\nu z) \sim \frac{i2}{(2\pi\nu)^{\frac{1}{2}}} \left[1 - \frac{\alpha^2}{\gamma^2}\left(1 + \frac{y}{R_o}\right)^2\right]^{-\frac{1}{4}}$$

$$\left\{ e^{\gamma k_o R_o f(\frac{\alpha}{\gamma})}\, e^{-k_o \lambda y (1-\frac{\alpha^2}{\gamma^2})^{\frac{1}{2}}} - \frac{i}{2} e^{-\gamma k_o R_o f(\frac{\alpha}{\gamma})}\, e^{k_o \lambda y (1-\frac{\alpha^2}{\gamma^2})^{\frac{1}{2}}} \right\} \tag{3.9}$$

to $O(\frac{1}{\nu})$.

With the definitions

$$\lambda \triangleq (\gamma^2 - \alpha^2)^{\frac{1}{2}} \tag{3.10a}$$

and

$$F(\lambda) \triangleq \gamma \tilde{f}(\tfrac{\alpha}{\gamma}) = \gamma \tanh^{-1}(\tfrac{\lambda}{\gamma}) - \lambda \tag{3.10b}$$

(3.9) gives (recall $k_o R_o >> 1$)

$$\frac{H_\nu^{(2)}(k_o\alpha r)}{H_\nu^{(2)}(k_o\alpha R_o)} \sim e^{-k_o\lambda y} - ie^{-2k_oR_oF(\lambda)} \sinh(k_o\lambda y) \tag{3.10c}$$

where we have also used $r = R_o + y$.

Using (3.4a) with (3.6), (3.7), and (3.8), we find

$$J_\nu(k_o\alpha r) \sim \frac{\left[1 - \frac{\alpha^2}{\gamma^2}(1 + \frac{y}{R_o})^2\right]^{-\frac{1}{4}}}{(2\pi\nu)^{\frac{1}{2}}} e^{k_o\lambda y(1-\frac{\alpha^2}{\gamma^2})^{\frac{1}{2}}} e^{-\gamma k_o R_o f(\frac{\alpha}{\gamma})} \tag{3.11}$$

to $O(\frac{1}{\nu})$. Employing (3.11) we find directly

$$\frac{J_\nu(k_o\alpha r)}{J_\nu(k_o\alpha R_o)} \sim e^{k_o\lambda y} \tag{3.12}$$

Also, using (3.9) and (3.11) we have

$$J_\nu(k_o\alpha R_o)H_\nu^{(2)}(k_o\alpha R_o) \sim \frac{1}{\pi k_o R_o \lambda}\left\{\frac{1}{2} e^{-2\gamma k_o R_o f(\frac{\alpha}{\gamma})} + i\right\} \tag{3.13}$$

We now have each of the elemental results necessary for finding an asymptotic representation for $J_\nu(k_o\alpha r')H_\nu^{(2)}(k_o\alpha r)$. From (3.10c) and (3.12) we have

$$J_\nu(k_o\alpha r')H_\nu^{(2)}(k_o\alpha r) \sim J_\nu(k_o\alpha R_o)H_\nu^{(2)}(k_o\alpha R_o)e^{y'k_o\lambda}$$

$$\left\{ e^{-k_o\lambda y} - i\, e^{-2k_oR_oF(\lambda)} \sinh(k_o\lambda y) \right\} \tag{3.14}$$

Finally, substitution of (3.13) in (3.14) yields our objective,

$$J_\nu(k_o\alpha r')H_\nu^{(2)}(k_o\alpha r) \sim \frac{1}{\pi k_oR_o} \left\{ \frac{i}{\lambda} e^{-k_o\lambda(y-y')} + \frac{1}{2\lambda} e^{k_o\lambda(y+y')} e^{-2k_oR_oF(\lambda)} \right\} + O(\tfrac{1}{\nu^2}) \tag{3.15}$$

where terms of $O\,(e^{-4k_oR_oF(\lambda)})$ have been neglected.

3.2.3 The Modified Integral Representations of V_e, V_m

Using results (3.3a), (3.3b) and (3.15) in (2.46a) and (2.46b) as well as (2.48a) and (2.48b), the ancillary potentials V_e and V_m seen to be separable into primary and secondary components; i.e., we may write $V_e = V_e^p + V_e^s$, $V_m = V_m^p + V_m^s$, where

$$V_e^p(y,y',z,z') = \left(\frac{-\zeta_o}{n_2^2}\right) \frac{1}{4\pi k_oR_o} \int_{\gamma_{1,2}} \frac{e^{-k_o\lambda(y-y')}}{\lambda} \frac{\alpha d\alpha}{u_2} \{-\} \tag{3.16a}$$

$$V_e^s(y,y',z,z') = \left(\frac{i\zeta_o}{n_2^2}\right) \frac{1}{8\pi k_oR_o} \int_{\gamma_{1,2}} \frac{e^{k_o\lambda(y+y')}\, e^{-2k_oR_oF(\lambda)}}{\lambda} \frac{\alpha d\alpha}{u_2} \{-\} \tag{3.16b}$$

$$V_m^p(y,y',z,z') = \left(\frac{-i}{4\pi R_o}\right) \int_{\gamma_{1,2}} \frac{e^{-k_o\lambda(y+y')}}{\lambda} \frac{\alpha d\alpha}{u_2} \{-\} \tag{3.16c}$$

$$V_m^s(y,y',z,z') = \left(\frac{-1}{8\pi R_o}\right) \int_{\gamma_{1,2}} e^{k_o\lambda(y+y')}\, e^{-2k_oR_oF(\lambda)} \frac{\alpha d\alpha}{u_2} \{-\} \tag{3.16d}$$

For convenience we have omitted detailed representation of those portions of the integrands which remain unchanged as the result of applying the Debye expansions. Classification of terms as primary or secondary components is made on the basis of the fact that in the limit as $R_o \to \infty$, $R_o V_e^p$ and $R_o V_m^p$ approach the forms assumed by the ancillary potentials in the straight guide case. Because of the presence of the factor $e^{-2k_o R_o F(\lambda)}$, choice of the proper branch of λ will in general yield $V_e^s << V_e^p$ and $V_m^s << V_m^p$; indeed, both $R_o V_e^s$ and $R_o V_m^s$ vanish as $R_o \to \infty$.

Despite the fact that the secondary ancillary potentials are much smaller in magnitude than their primary counterparts, V_e^s and V_m^s are the terms of interest for our purposes here. This follows from the fact that, in addition to their relatively small magnitudes when compared to the primary potentials, both V_e^s and V_m^s exhibit an exponentially increasing character for increasing y, and each stands in quadrature to its associated primary potential. These features of V_e^s and V_m^s allow an association between these secondary potentials and the electric and magnetic fields exterior to the bent channelguide which have been reflected from the caustic; i.e., the electric and magnetic fields derivable from the secondary, ancillary potentials V_e^s and V_m^s are the fields $\delta\bar{E}$ and $\delta\bar{H}$, respectively.

We will henceforth focus attention on the ancillary potentials V_e^s of (3.16b) and V_m^s of (3.16d) in order to characterize the radiation from the bent channel guide. Because of the linearity of all operators involved, equation (2.49) still applies and the components produced are the z-components of $\delta\bar{E}$ and $\delta\bar{H}$.

3.3 The Asymptotic Form of V_e^s

3.3.1 A Change of Variables

To assure convergence of our fundamental integral representations of V_e and V_m, we have chosen to employ the branches of $u_1 = (\alpha^2 - n_1^2)^{\frac{1}{2}}$ and $u_2 = (\alpha^2 - n_2^2)^{\frac{1}{2}}$ for which $\text{Re}\, u_1 > 0$, $\text{Re}\, u_2 > 0$. It is in connection with these branches of u_1 and u_2 that the branch cuts at n_1 and n_2 arise in the α-plane. The contours γ_1 and γ_2 follow the branch cuts at n_1 and n_2, respectively, and it follows from the same analysis that specifies the branch cuts (not discussed herein) that u_1 is purely imaginary along γ_1 and u_2 is purely imaginary along λ_2. Indeed, if we consider γ_2 to be composed of segments $\gamma_{2\ell}$, g_2, γ_{2u} (i.e., $\gamma_2 = \gamma_{2\ell} + g_2 + \gamma_{2u}$) it is possible to show that $\arg u_2 = -\frac{\pi}{2}$ on $\gamma_{2\ell}$ and $\arg u_2 = \frac{\pi}{2}$ on γ_{2u} (cf. Figure 3.2). The segment g_2 is a circular segment centered on n_2 whose radius we allow to vanish, whereupon we find no contribution from g_2 to the integrals over γ_2 in (3.16b) and (3.16d). Analogous statements follow for the argument of u_1 on γ_1, with $\gamma_1 = \gamma_{1\ell} + g_1 + \gamma_{1u}$, and for the contribution from g_1 to the integrals over γ_1 in (3.16b) and (3.16d).

Analysis shows that we may select a branch of the function $(n_2^2 - \alpha^2)^{\frac{1}{2}}$ consistent with the extant branch cut at n_2 such that $\text{Im}(n_2^2 - \alpha^2)^{\frac{1}{2}} < 0$, thus we may write

$$u_2 = i s_2 \tag{3.17a}$$

where

$$s_2 = (n_2^2 - \alpha^2)\,, \quad \text{Im}(n_2^2 - \alpha^2)^{\frac{1}{2}} < 0 \tag{3.17b}$$

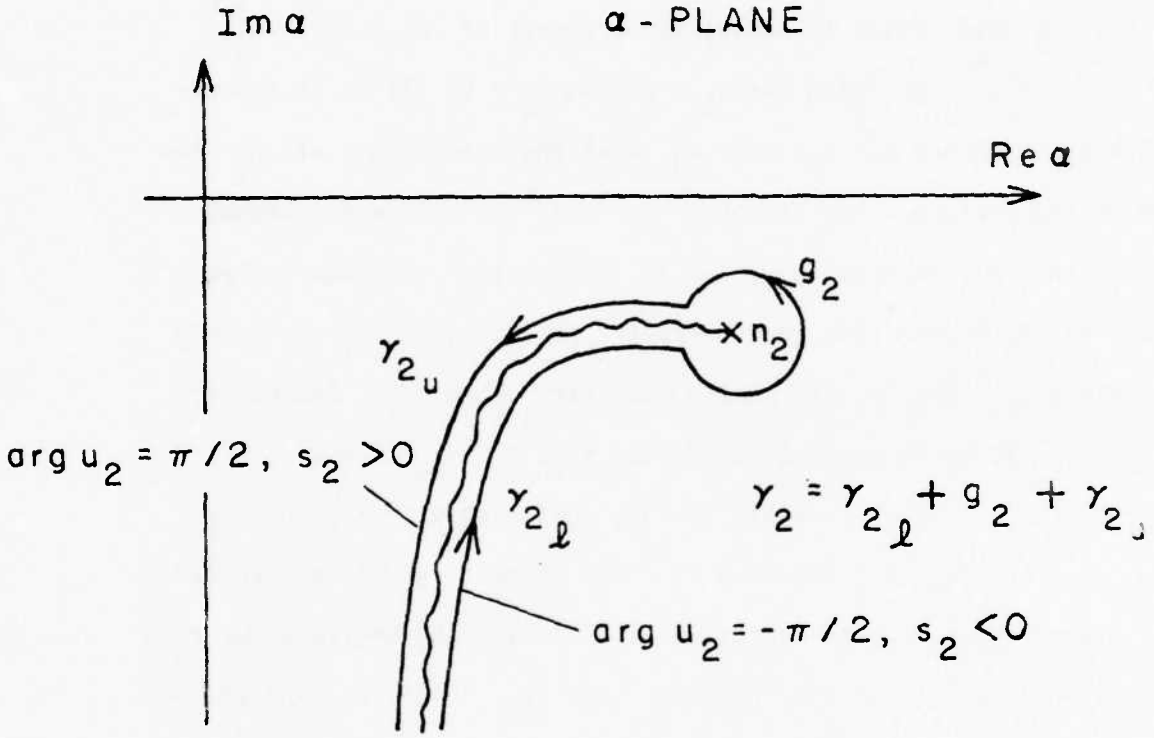

Figure 3.2 A Close-Up of Contour γ_2

Since u_2 is purely imaginary along $\gamma_{2\ell}$ and γ_{2u}, then s_2 must be purely real along these same segments. Indeed, the nature of u_2 along $\gamma_{2\ell}$ and γ_{2u} along with (3.17a) requires s_2 real and $s_2 < 0$ on $\gamma_{2\ell}$ and s_2 real and $s_2 > 0$ along γ_{2u} (cf. Figure 3.2). Thus, a change of variables from α to s_2 in (3.16b) and (3.16d) using (3.17a) will convert integrals along γ_2 in the α-plane to integrals along the full extent of the real axis ($-\infty$ to $+\infty$) in the s_2-plane. In the same way, one may write

$$u_1 = i s_1 \tag{3.18a}$$

where

$$s_1 = (n_1^2 - \alpha^2)^{\frac{1}{2}}, \quad \mathrm{Im}(n_1^2 - \alpha^2)^{\frac{1}{2}} < 0 \tag{3.18b}$$

as a change of variables from α to s_1 in (3.16b) and (3.16d) to convert integrals over γ_1 in the α-plane to integrals over the full extent of the real axis in the s_1-plane.

For the purpose of illustration, we will consider that portion of V_e^s obtained from integration over the contour γ_2, while noting that an analogous procedure may be performed for that portiom of v_e^s obtained from integration over γ_1. At the end of this chapter we will see, in fact, that the contribution to V_e^s due to the integration over γ_1 can be neglected because of its insignificant amplitude relative to the contribution arising from the integration over γ_2.

From (3.17a) and (3.17b) we have $\frac{ds_2}{d\alpha} = -i\alpha(\alpha^2 - n_2^2)^{-\frac{1}{2}}$, so

$$ds_2 = -i \frac{\alpha d\alpha}{u_2} \tag{3.19}$$

Recalling λ from (3.10a) and using (3.17a) and (3.17b), we may write

$$\lambda = (\lambda_2^2 + s_2^2)^{\frac{1}{2}} \tag{3.20a}$$

where

$$\lambda_2^2 = \gamma^2 - n_2^2 \tag{3.20b}$$

Also, we may write

$$u_1 = (\nu_2^2 - s_2^2)^{\frac{1}{2}} \tag{3.21a}$$

where

$$\nu_2^2 = n_2^2 - n_1^2 \tag{3.21b}$$

Using (3.19), (3.20a), (3.20b), (3.21a), and (3.21b) in (3.16b), we have

$$V_e^s(y,y',z,z') = \left(\frac{-\zeta_o}{8\pi n_2^2 k_o R_o}\right) \int_{-\infty}^{\infty} T_e(y,y',z,z';s_2) e^{k_o R_o q_2(s_2)} ds_2 \tag{3.22a}$$

where

$$T_e(y,y',z,z';s_2) = \frac{e^{k_o\lambda(y+y')}}{\lambda} \quad \frac{2u_2 n_2^2}{u_1 n_2^2 + u_2 n_1^2} \quad e^{k_o(u_2 z' - u_1 z)}, \qquad z \geq 0 \tag{3.22b}$$

$$T_e(y,y',z,z';s_2) = \frac{e^{k_o\lambda(y+y')}}{\lambda} \quad \frac{u_2 n_1^2 - u_1 n_2^2}{u_1 n_2^2 + u_2 n_1^2} e^{k_o u_2 (z+z')} + e^{-k_o u_2 |z-z'|}, \qquad z \leq 0 \tag{3.22c}$$

where $u_2 = is_2$, $u_1 = (\nu_2^2 - s_2^2)^{\frac{1}{2}}$, and

$$q_2(s_2) = 2\left\{\frac{\gamma}{2} \log \frac{\gamma-\lambda}{\gamma+\lambda} + \lambda\right\}, \quad \lambda = (\lambda_2^2 + s_2^2)^{\frac{1}{2}} \tag{3.22d}$$

3.3.2 Evaluation of V_e^s

Since we assume $k_o R_o >> 1$, the form of V_e^s given in (3.22a) lends itself readily to a steepest descent type of asymptotic evaluation (cf. [7]).

Proceeding as outlined in Appendix B we find

$$V_e^s(y,y',z,z') \sim \frac{-\zeta_o}{16\pi^2 n_2^2 k_o R_o} \left(\frac{\pi n_2^2}{\lambda_2 k_o R_o} \right)^{3/2} e^{k_o R_o q_2(0)}$$

$$\frac{e^{\lambda_o \lambda_2 (y+y')}}{\lambda_2} \left[k_o z' - \frac{n_1^2}{n_2^2 (n_2^2 - n_1^2)^{\frac{1}{2}}} \right] \left[k_o z - \frac{n_1^2}{n_2^2 (n_2^2 - n_1^2)^{\frac{1}{2}}} \right] \quad (3.23)$$

A similar result is obtained for the component of V_e^s derived by integration over γ_1. However, consider the series representation of $q_1(0)$ and $q_2(0)$ derived by expanding their logarithmic terms [cf. (3.22d)]

$$q_i(0) = -2\gamma \sum_1^\infty \frac{1}{(2n+1)} \left(\frac{\lambda_i}{\gamma} \right)^{2n+1} \quad (3.24)$$

where

$$\left(\frac{\lambda_i}{\gamma} \right) = \left(1 - \frac{n_i^2}{\gamma^2} \right)^{\frac{1}{2}} , \quad i = 1,2 .$$

For $q_1(0)$, $\left(\frac{n_1}{\gamma} \right)^2 << 1$, so $\left(\frac{\lambda_1}{\gamma} \right) \approx 1$,

whereas for $q_2(0)$, $\left(\frac{n_2}{\gamma} \right)^2 \approx 1$, so $0 < \left(\frac{\lambda_2}{\gamma} \right) << 1$. For typical integrated optics material parameters then, (3.24) gives $|q_1(0)| >> |q_2(0)|$ so that $e^{k_o R_o q_1(0)} << e^{k_o R_o q_2(0)}$ and we are justified in neglecting the contribution from the integration over contour γ_1.

CHAPTER 4

RADIATION LOSS FROM A CURVED RECTANGULAR CHANNEL GUIDE FAR FROM CUTOFF

4.1 Introduction

As discussed briefly in Chapter 1, we will know the continuous radiation loss from a section of curved dielectric channel waveguide once we have found the normalized attenuation constant α as given by (1.2). Evaluation of α requires computation of the quantities P and c in (1.3) and (1.4), respectively. Our efforts in Chapters 2 and 3 have been to derive an expression from which we can determine the caustic-reflected fields $\delta\overline{E}$ and $\delta\overline{H}$ in terms of the straight channel fields. Equations (2.49) and (3.23) allow us now to do so. Thus, we are left with the task of specifying the straight channel fields $\overline{E}_o$, $\overline{H}_o$ for any case of practical interest and using these with (2.49), (3.23), (1.2), and (1.3) in order to find α.

The general problem of determining the fields within a straight, rectangular dielectric channel waveguide embedded in a substrate has not been rigorously solved analytically. However, an approximate analytical method has been developed by Marcatili (cf. [2]) which yields straight channel field expressions which are valid for well confined channel modes, i.e., channel modes that are far from cutoff. We will employ Marcatili's results and thus generate an expression for the radiation from a curved dielectric channel waveguide with associated straight channel modes that are far from cutoff. In particular, we consider the straight, rectangular

dielectric channel waveguide configuration of Fig. 4.1 which illustrates the general disposition of material regions to which Marcatili's analytical procedure can be applied. The material parameters assigned to the various regions are consistent with those of the associated curved channel guide problem illustrated in Figure 1.2. The assumption of propagating modes that are far from cutoff and therefore highly confined within the channel region is extended by the stipulation that the fields in the shaded regions of Figure 4.1 are negligible, hence no material parameters need be specified there.

It should also be noted that the origin of the (x,w,s) coordinate system is off-set from the local cartesian system (x,y,s) in Figure 1.1. To convert to the (x,w,s) system from the (x,y,s) system we need only employ the transformation

$$y = w - \frac{b}{2} \tag{4.1}$$

The structure of Figure 4.1 can support a set of modes that are predominantly x-polarized and are designated E^x_{pq} modes. In addition, such a structure can also support a set of modes that are predominantly y-polarized and are designated E^y_{pq} modes. Although such a structure can support both modes, we consider only radiation due to the E^x_{pq} modes whose field distributions in the channel guide are given by Marcuse (cf. [11])

$$E_{os} = A \cos k_x(x + \xi)\cos k_w(w+\eta) \tag{4.2a}$$

$$E_{ox} = \frac{iA}{\beta} \frac{n^2k_o^2 - k_x^2}{k_x} \sin k_x(x+\xi)\cos k_w(w+\eta) \tag{4.2b}$$

$$E_{ow} \simeq 0 \tag{4.2c}$$

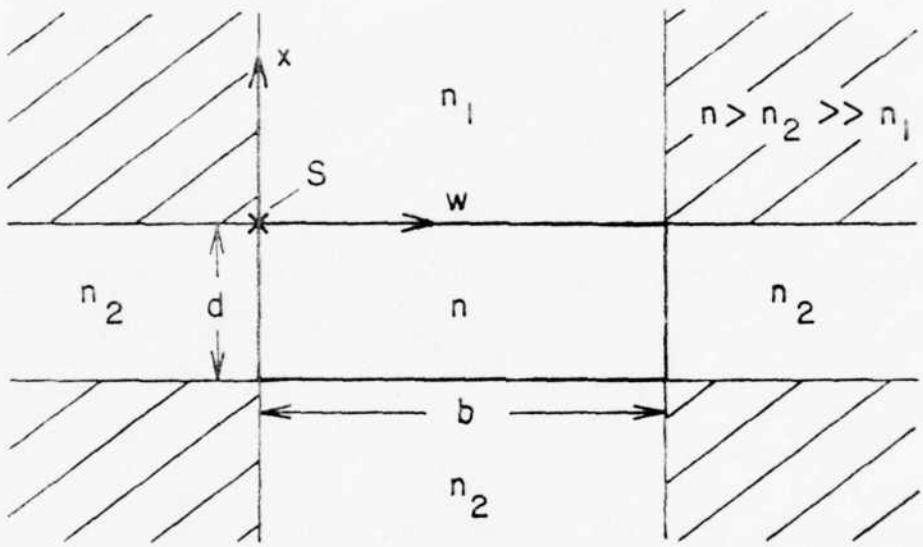

Figure 4.1 The Straight, Rectangular Dielectric Channel Waveguide Configuration

$$H_{os} = -A\left(\frac{n^2}{\zeta_o}\right)\left(\frac{k_w}{k_x}\right)\left(\frac{k_o}{\beta}\right) \sin k_x(x+\xi)\sin k_w(w+\eta) \tag{4.2d}$$

$$H_{ox} \equiv 0 \tag{4.2e}$$

$$H_{ow} = iA\left(\frac{k_o n}{k_x \zeta_o}\right) \sin k_x(x+\xi)\cos k_w(w+\eta) \tag{4.2f}$$

where $k_o = w\sqrt{\mu_o \varepsilon_o}$ is the free-space phase constant, β is the phase constant of the fields in the channel (propagation of the form $e^{i(wt-\beta s)}$ is assumed), and $\zeta_o = \sqrt{\frac{\mu_o}{\varepsilon_o}}$ is the free-space wave impedance. The parameters k_x and k_w are separation constants related by

$$n^2 k_o^2 - \beta^2 = k_x^2 + k_y^2 \tag{4.3}$$

and are solutions of the eigenvalue equations

$$\tan k_x d = \frac{n^2 k_x (n_1^2 \gamma_2 + n_2 \gamma_3)}{(n_1^2 n_2^2 k_x^2 - n^4 \gamma_2 \gamma_3)} \tag{4.4a}$$

$$\tan k_w b = \frac{2k_w \gamma_4}{(k_w^2 - \gamma_4^2)} \tag{4.4b}$$

The parameters γ_j are given by

$$\gamma_2 = [(n^2 - n_2^2)k_o^2 - k_x^2]^{\frac{1}{2}} \tag{4.5a}$$

$$\gamma_3 = [(n^2 - n_1^2)k_o^2 - k_x^2]^{\frac{1}{2}} \tag{4.5b}$$

$$\gamma_4 = [(n^2 - n_2^2)k_o^2 - k_w^2]^{\frac{1}{2}} \tag{4.5c}$$

(3.18a)

The parameters γ_j are transverse decay constants of the fields in the material regions below, above, and on either side of the region of refractive index n (the channel guide), respectively; e.g., the fields in the material region below the channel guide region decay like $e^{\gamma_2(x+d)}$, $x \leq -d$. It follows that each of the parameters γ_j satisfies $\gamma_j > 0$.

Once k_x and k_w are known, the phase parameters ξ and η are determined from

$$\tan k_x \xi = - \left(\frac{n_1}{n}\right)^2 \frac{k_x}{\gamma_3} \tag{4.6a}$$

$$\tan k_w \eta = -\frac{\gamma_4}{k_w} \tag{4.6b}$$

Also, notice that once k_x and k_w are known, (4.2) may be solved to yield β.

4.2 Expressions for P and C

Application of the assumption of modes far from cutoff and employing the local coordinate representations for the field components allows (1.3) and (1.4) to be rewritten, respectively, as

$$P = 2\int_{-d}^{o} dx \int_{o}^{b} dy(E_{ox}H_{ow}) \tag{4.7}$$

$$C = \int_{-d}^{o} \left\{ \bar{E}_o^- \times \delta\bar{H} - \delta\bar{E} \times \bar{H}_o^- \right\} \cdot \bar{a}_w dx \Big|_{w=b} \tag{4.8}$$

As discussed in detail in Appendix C, the straight channel field expressions (4.2) may be used with the ancillary potential V_e^s from (3.23) in (4.7), and (4.8) to evaluate P and C as

$$P = -2A^2 \left[\frac{n^2k_o^2 - k_x^2}{k_x^2}\right] \frac{k_o n^2}{\beta\zeta_o} \left(\frac{d}{2} + L_x\right)\left(\frac{b}{2} + L_w\right) \tag{4.9}$$

$$C = -A^2 C_1 C_2^2 \, \mathrm{sgn}[\cos(k_w b)]\mathrm{sgn}[k_w^2 - \gamma_4^2]$$

$$\left[\frac{k_w k_o (n^2k_o^2 - k_x^2)(n^2 - n_2^2)^{\frac{1}{2}}}{16\pi^2\beta^2 k_x^2 \lambda_2 \zeta_o}\right] \left[\lambda_2(n^2k_o^2 - k_x^2) + n^2 k_o \gamma_4\right]$$

$$\left(\frac{\pi n_2^2}{k_o R_o \lambda_2}\right)^{3/2} e^{(k_o\lambda_2 b)/2} \, e^{k_o R_o q_2(0)} \tag{4.10}$$

where the constants L_x, L_w, C_1, and C_2 are given in Appendix C as equations (C.5a), (C.5b), (C.22), and (C.25), respectively.

4.3 The Evaluation of α

The normalized attenuation constant is given in (1.2). Before evaluating α in terms of (4.9) and (4.10), it is advantageous to normalize C_1, C_2, and $A_e \triangleq \left(\frac{d}{2} + L_x\right)\left(\frac{b}{2} + L_w\right)$ to k_o. Doing this we have

$$C_1 = \frac{\nu_w}{k_o \Gamma_2^2 (n^2 - n_2^2)^{\frac{1}{2}}} \left\{ \lambda_2 [\mathrm{sgn}[\cos(k_o b)\nu_w]\mathrm{sgn}[\nu_w^2 - \Gamma_4^2]\right.$$

$$e^{(k_o b)\lambda_2/2} - e^{-(k_o b)\lambda_2/2}\Big] + \Gamma_4 \Big[\mathrm{sgn}[\cos(k_o b)\nu_w]$$

$$\mathrm{sgn}[k_o^2(\nu_y^2 - \Gamma_4^2)]\, e^{(k_o b)\lambda_2/2} + e^{(k_o b)\lambda_2/2}\Big]\Big\} \tag{4.12}$$

$$C_2 = \frac{1}{k_o \nu_x}\Bigg\{\Bigg[\mathrm{sgn}[\cos(k_o d)\nu_x]\ \mathrm{sgn}[(n_1^2 n_2^2 \nu_x^2 - n^4 \Gamma_2 \Gamma_3)]$$

$$\frac{(n^2\Gamma_2(k_o d) + n_2^2)}{(n_2^4\nu_x^2 + n^4\Gamma_2^2)^{\frac{1}{2}}}\Bigg] + \frac{n^2 n_1^2}{n_2^2(n_2^2 - n_1^2)^{\frac{1}{2}}}$$

$$\Bigg[\frac{\Gamma_3}{(n^4\Gamma_3^2 + n_1^4\nu_x^2)^{\frac{1}{2}}} + \mathrm{sgn}[\cos(k_o d)\nu_x]\mathrm{sgn}[k_o^2(n_1^2 n_2^2 \nu_x^2 - n^4\Gamma_2\Gamma_3)]$$

$$\frac{\Gamma_2}{(n_2^4\nu_x^2 + n^4\Gamma_2^2)^{\frac{1}{2}}}\Bigg]\Bigg\} \tag{4.13}$$

$$A_e = \frac{1}{4k_o^2}\Bigg\{\Bigg((k_o d) + n^2\ \Bigg[\frac{n_1^2\Gamma_3}{(n_1^4\nu_x^2 + n^4\Gamma_3^2)} + \frac{n_2^2\Gamma_2}{(n_2^2\nu_x^2 + n^4\Gamma_2^2)}\Bigg]\Bigg)$$

$$\Bigg((k_o b) + \frac{2\Gamma_4}{(n^2 - n_2^2)}\Bigg)\Bigg\} \tag{4.14}$$

where

$$\nu_i = K_i/k_o \tag{4.15a}$$

$$\Gamma_i = \gamma_i/k_o \tag{4.15b}$$

With (4.12), (4.13), (4.14) and (4.9), (4.10) in (1.2) we find

$$\alpha = -\mathrm{sgn}[\cos(k_o b)\nu_w]\ \mathrm{sgn}[\nu_w^2 - \Gamma_4^2]\left(\frac{F_N}{F_D}\right) \tag{4.16a}$$

where

$$F_N = \left\{ \frac{n_2^3}{n^2} \left(\frac{\nu_w}{\nu_x} \right)^2 \left[\lambda_2 (\mathrm{sgn}[\cos(k_o b)\nu_w]) \mathrm{sgn}[\nu_w^2 - \Gamma_4^2] \right.\right.$$

$$e^{(k_o b)\lambda_2/2} - e^{-(k_o b)\lambda_2/2}) + \Gamma_4 (\mathrm{sgn}[\cos(k_o b)\nu_w]$$

$$\left.\left. \mathrm{sgn}[\nu_w^2 - \Gamma_4^2]\, e^{(k_o b)\lambda_2/2} + e^{-(k_o b)\lambda_2/2}) \right] \right] \left[\mathrm{sgn}[\cos(k_o d)\nu_x] \right.$$

$$\mathrm{sgn}[n_1^2 n_2^2 \nu_x^2 - n^4 \Gamma_2 \Gamma_3] \frac{(n^2 \Gamma_2 (k_o d) + n_2^2)}{(n_2^4 \nu_x^2 + n^4 \Gamma_2^2)^{1/2}} - \frac{n_1^2}{(n^4 \Gamma_3^2 + n_1^4 \nu_x^2)^{1/2}}$$

$$+ \frac{n^2 n_1^2}{n_2^2 (n_2^2 - n_1^2)^{1/2}} \left(\frac{\Gamma_3}{(n^4 \Gamma_3^2 + n_1^4 \nu_x^2)^{1/2}} + \mathrm{sgn}[\cos(k_o d)\nu_x] \right.$$

$$\left.\left. \mathrm{sgn}[n_1^2 n_2^2 \nu_x^2 - n^4 \Gamma_2 \Gamma_3] \frac{\Gamma_2}{(n_2^4 \nu_x^2 + n^4 \Gamma_2^2)^{1/2}} \right) \right]^2$$

$$\left. [\lambda_2 (n^2 - \nu_x^2) + n^2 \Gamma_4]\, e^{(k_o b)\lambda_2/2} \left[\frac{e^{(k_o R_o) q_2(0)}}{(k_o R_o)^{3/2}} \right] \right\} \qquad (4.16b)$$

$$F_D = \left\{ (8\pi^{1/2} \lambda_2^{5/2} \gamma_o \Gamma_2^2) \left[(k_o b) + \frac{2\Gamma_4}{(n^2 - n_2^2)} \right] \right.$$

$$\left. \left[(k_o d) + n^2 \left(\frac{n_1^2 \Gamma_3}{n_1^4 \nu_x^2 + n^4 \Gamma_3^2)} + \frac{n_2^2 \Gamma_2}{n_2^4 \nu_x^2 + n^4 \Gamma_2^2} \right) \right] \right\} \qquad (4.16c)$$

and where

$$\gamma_o = \beta / k_o = [n^2 - (\nu_x^2 + \nu_y^2)]^{1/2} \qquad (4.17a)$$

$$\lambda_2 \approx (\gamma_o^2 - n_2^2)^{1/2} \qquad (4.17b)$$

In order to highlight the dependence of this cumbersome result on the radius of curvature of the channel we simplify (4.16a) through (4.16c) by writing

$$\alpha = \frac{C_i}{(k_o R_o)^{3/2}} \; e^{k_o R_o q_2(0)} \tag{4.18}$$

where C_i (the subscript i designating that this result is associated with an "inhomogeneous" medium about the channel guide) is a parameter dependent upon the refractive indices of the channel guide and its surrounding media, the dimensions of the channel guide, and the specific E^x_{pq} mode propagating in the channel.

Figure 4.2 is a plot of the normalized attenuation coefficient versus $k_o R_o$ for $k_o d = 5$ and $k_o b = 10$. The refractive index of the channel guide is assigned to be 4.04, that of the substrate 4.00, and that of the covering medium 1.00.

4.4 Conclusions

As mentioned in Secion 1.1, there are no analytical reports in the literature which address a problem similar enough to that considered here to allow comparisons with the force to effectively confirm or reject the principal result derived in this report, i.e., the form of the normalized attenuation coefficient α presented in Section 4.4. To this extent, then, the expression for α in (4.16) is a new result. To appreciate that the form of α constitutes a unique as well as a new result, we consider the form of the normalized attenuation coefficient α' (primes do not indicate differentiation here) for a bent, rectangular dielectric waveguide immersed in a homogeneous medium of lower refractive index than that of the guide (cf. [5], Section 9.8), i.e.

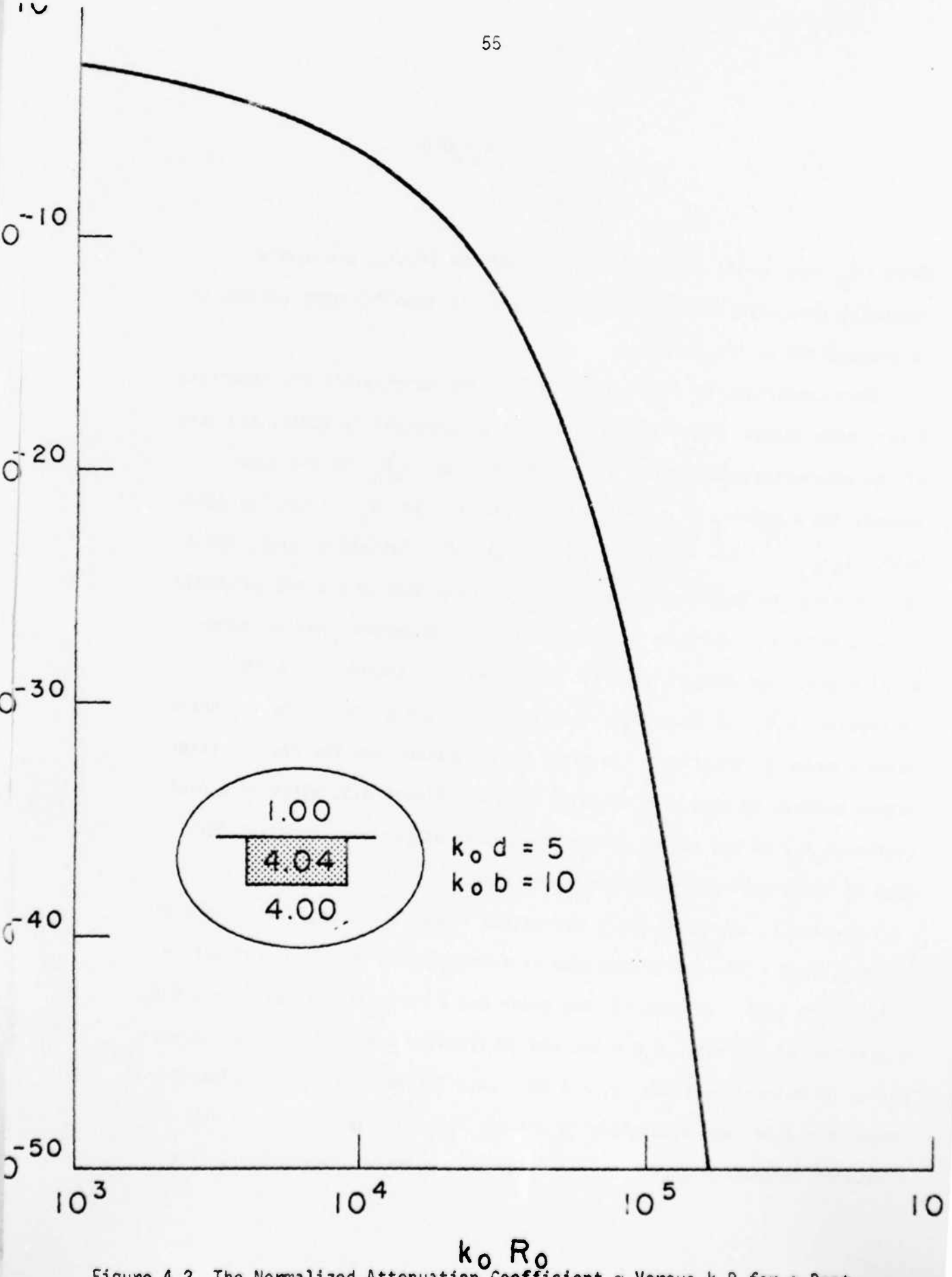

Figure 4.2 The Normalized Attenuation Coefficient α Versus $k_o R_o$ for a Bent, Rectangular Channel Guide in a Dense Substrate

$$\alpha' = \frac{C_h}{(k_o R_o)^{\frac{1}{2}}} \; e^{k_o R_o Q(0)} \tag{4.19}$$

where C_h and $Q(0)$, like C_i and $q_2(0)$ in (4.41), are parameters depending upon material characteristics and the specific mode assumed to be propagating in the guide.

Upon comparison of (4.19) with (4.18), two conclusions are immediate. First, even though $Q(0)$ and $q_2(0)$ are not necessarily equal, the form of the exponential dependence of α and α' on $k_o R_o$ is the same. Second, the algebraic dependence of α and α' on R_o is not the same, being $(\frac{1}{k_o R_o})^{3/2}$ for α and $(\frac{1}{k_o R_o})^{\frac{1}{2}}$ for α'. Certainly, then, for a pair of bent, rectangular dielectric waveguides, one in a dense substrate below a material interface and the other in a homogeneous medium, when $q_2(0) = Q(0)$, one expects the rate of decrease of attenuation with increasing $k_o R_o$ to be greater in the case of the guide in the substrate below a material interface. In order to understand how the overall attenuation behaves in such situations we consider Figure 4.3, which is a plot (versus $k_o R_o$) of the values of the normalized attenuation constant for each of three bent waveguide configurations.

In case I, the guide has a refractive index $n = 4.04$, dimensions of $k_o d = 3$, $k_o b = 10$, and is embedded in a homogeneous medium of refractive index $n_1 = 4.00$. In case II, the guide has a refractive index $n = 4.028$, dimensions of $k_o d = 5$, $k_o b = 10$, and is likewise embedded in a homogeneous medium of refractive index $n_1 = 4.00$. Case III has a guide of refractive index $n = 4.04$ and dimensions $k_o d = 5$, $k_o b = 10$ embedded in a substrate of refractive index $n_2 = 4.00$ below a material region refractive

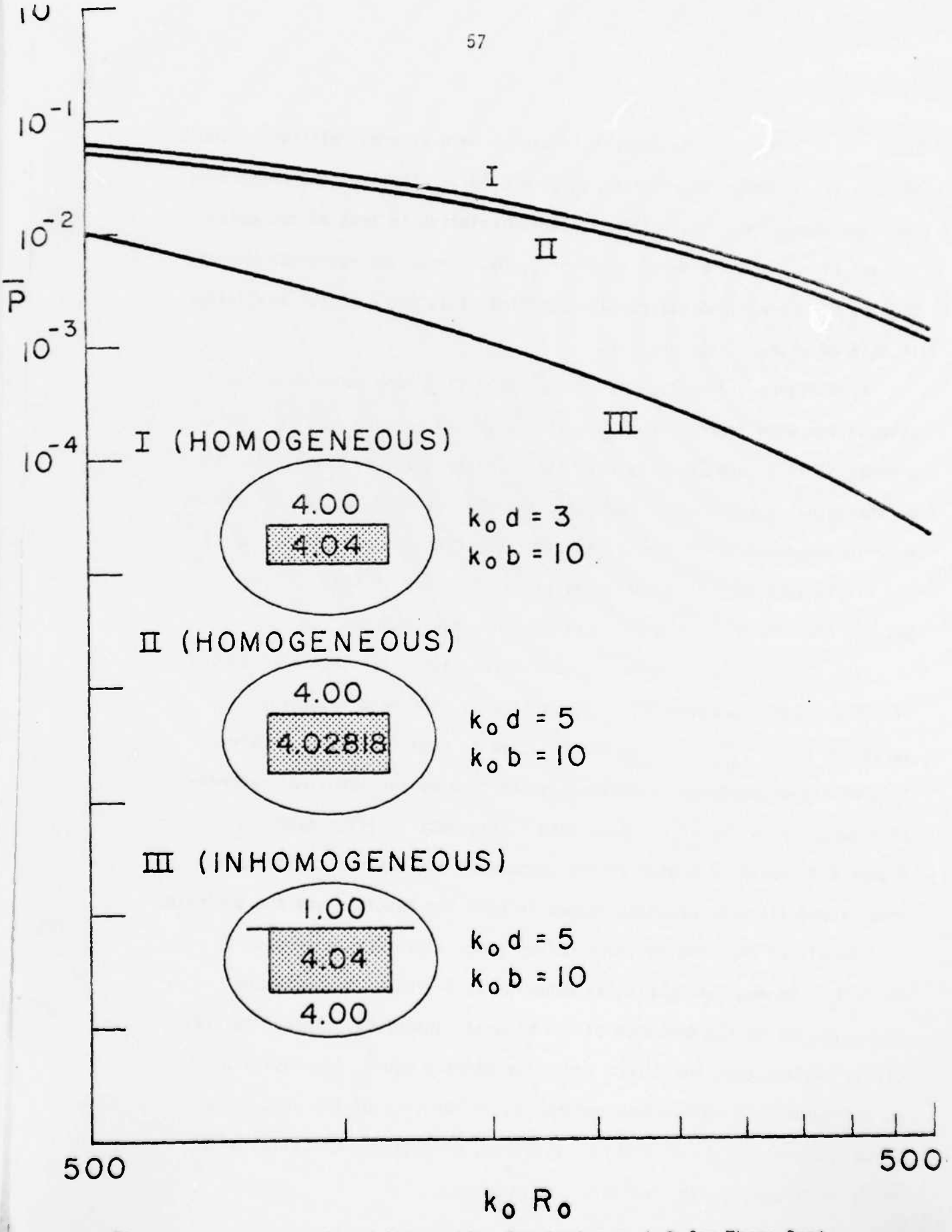

Figure 4.3 The Normalized Attenuation Constant v.s. $k_o R_o$ for Three Bent Waveguide Configurations with Identical Exponential Variation

index $n_1 = 1.00$. The dimensions in case I were altered relative to those of case III in order to provide $q_2(0) = Q_I(0)$. Likewise, the refractive index of the guide in case II was altered relative to that of the guide in case III to again assure $q_2(0) = Q_{II}(0)$. Thus, the exponential variation of the normalized attenuation coefficient is the same for the guides in each of cases I, II, and III.

From Figure 4.3 we see that in addition to a more rapid decrease in attenuation with increasing k_0R_0, the guide in a dense substrate below a material interface actually exhibits a lesser absolute attenuation than do the guides surrounded by homogeneous media. Indeed, while the difference in values of normalized attenuation constant between cases I or II and III is less than an order of magnitude for $k_0R_0 = 500$, it lies between one and two orders of magnitude for $k_0R_0 = 5000$.

The divergent tendency of the curve for case III relative to those of cases I and II results from the distinctly different algebraic variation with k_0R_0 in case III relative to cases I and II. However, this divergent tendency is ultimately overcome by the identical exponential decay terms present in each case. This fact is illustrated in Figure 4.4, which is a plot of the normalized attenuation constants for cases I and III over extended ranges in both the abscissa and the ordinate.

Recalling the inverse three-halves power algebraic dependence of α on k_0R_0, we may interpret this behavior as a kind of lateral-wave phenomenon due to the presence of the material interface. This interpretation implies that the direct radiation which accounts for losses of a curved guide in a homogeneous medium is, in the case of the guide in a dense substrate below a material interface, effectively cancelled by an image contribution from the material interface.

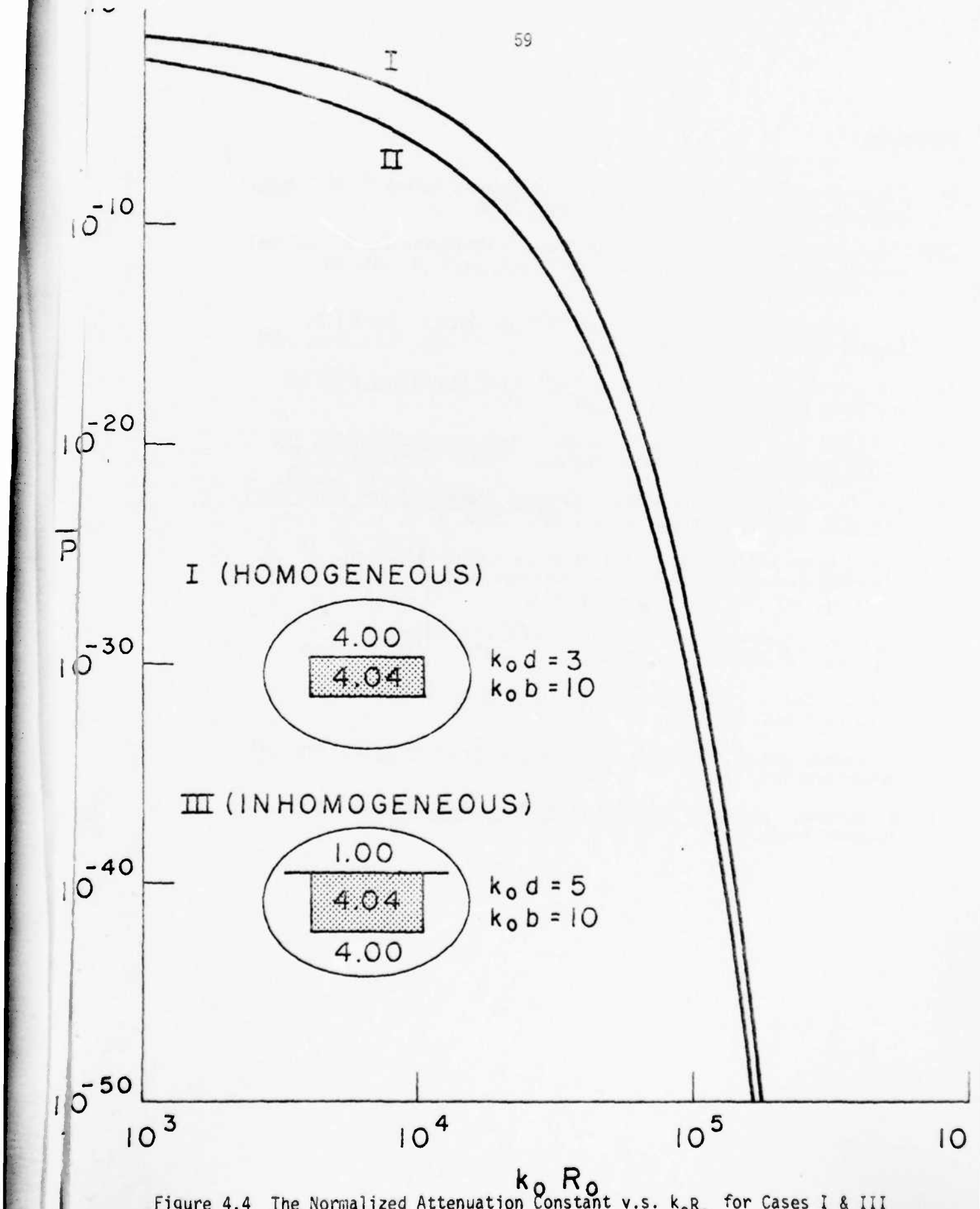

Figure 4.4 The Normalized Attenuation Constant v.s. k_oR_o for Cases I & III (Extended Range)

References

[1] E.A.J. Marcatili, "Bends in Optical Dielectric Guides," Bell Syst. Tech. J., vol. 48, pp. 2103-2132, Sept. 1969.

[2] E.A.J. Marcatili, "Dielectric Rectangular Waveguide and Directional Coupler for Integrated Optics," Bell Syst. Tech. J.,vol. 48, pp. 2071-2102, Sept. 1969.

[3] J.A. Arnaud, "Transverse Coupling in Fiber Optics - Part III; Bending Losses," Bell Syst. Tech. J. vol. 53, pp. 1379-1394, 1974.

[4] L.B. Felsen and N. Marcuvitz, Radiation and Scattering of Waves. Englewood Cliffs, NJ: Prentice Hall, 1973.

[5] L. Lewin, D.C. Chang and E.F. Kuester, Electromagnetic Waves and Curved Structures, Stevenage, England: Peter Peregrinus, 1977.

[6] V.A. Ditkin and A.O. Prudrikov, Integral Transforms and Operational Calculus, Oxford: Pergamon Press, 1965, chap. 3.

[7] R.H.T. Bates and F.L. Ny, "Polarization Source Formulation of Electromagnetism and Dielectric-Loaded Waveguides," Proc. IEE (London), vol. 119, pp. 1568-1574, 1972.

[8] G. Tyras, Radiation and Propagation of Electromagnetic Waves. New York: Academic Press, 1969.

[9] F.W.J. Olver, Asymptotics and Special Functions. New York: Academic Press, 1974.

[10] P. Dennery and A. Krzywicki, Mathematics for Physicists. New York, Harper and Row, 1967.

[11] D. Marcuse, Theory of Dielectric Optical Waveguides, New York: Academic Press, 1974.

Appendices

Appendix A

Determination and Application of Source and Boundary Conditions for $\tilde{\Phi}_r^e$, $\tilde{\Phi}_r^m$

A.1. Introduction

Inspection of (2.30a) through (2.30c) reveals that we have eight unknown transform coefficients, hence we expect to be able to specify eight independent equations relating these coefficients as determined by boundary and source conditions on the field components. We begin by considering equations (1.9a) through (1.9b) which relate the transforms of the fields transverse to the z-direction to the transforms of the cartesian field components. Direct integration of (1.9a) through (1.9b) after dividing both sides by α and multiplying through by $J_\nu(k_0\alpha r)$ gives the following results:

$$E_\phi(r,z) = i\zeta_0 \int_0^\infty \tilde{\Phi}_r^m(\alpha,z)J_\nu'(k_0\alpha r)d\alpha$$

$$\frac{-i\gamma R_0}{k_0 r}\int_0^\infty \frac{\partial}{\partial z}\tilde{\Phi}_r^e(\alpha,z)J_\nu(k_0\alpha r)\frac{d\alpha}{\alpha} \qquad \text{(A.1a)}$$

$$E_r(r,z) = \frac{-\zeta_0\gamma R_0}{r}\int_0^\infty \tilde{\Phi}_r^m(\alpha,z)J_\nu(k_0\alpha z)\frac{d\alpha}{\alpha}$$

$$+\frac{1}{k_0}\int_0^\infty \frac{\partial}{\partial z}\tilde{\Phi}_r^e(\alpha,z)J_\nu'(k_0\alpha r)d\alpha \qquad \text{(A.1b)}$$

$$H_\phi(r,z) = \frac{-i\gamma R_o}{rk_o}\int_o^\infty \frac{\partial}{\partial z}\,\tilde{\phi}_r^m(\alpha,z)J_\nu(k_o\alpha r)\frac{d\alpha}{\alpha}$$

$$\frac{-in_{1,2}^2}{\zeta_o}\int_o^\infty \tilde{\phi}_r^e(\alpha,z)J_\nu'(k_o\alpha r)d\alpha \qquad (A.1c)$$

$$H_r(r,z) = \frac{\gamma n_{1,2}^2 R_o}{r\zeta_o}\int_o^\infty \tilde{\phi}_r^e(\alpha,z)J_\nu(k_o\alpha r)\frac{d\alpha}{\alpha}$$

$$+\frac{1}{k_o}\int_o^\infty \frac{\partial}{\partial z}\,\tilde{\phi}_r^m(\alpha,z)J_\nu'(k_o\alpha r)d\alpha \qquad (A.1d)$$

A.2 Boundary Conditions at the Dielectric Interface

Since E_ϕ and E_r must be continuous at $z = 0$, inspection of (A.1a) and (A.1b) yields

$$\tilde{\phi}_r^m(\alpha,0+) = \tilde{\phi}_r^m(\alpha,0-) \qquad (A.2a)$$

$$\frac{\partial}{\partial z}\,\tilde{\phi}_r^e(\alpha,z)\Big|_{z=0+} = \frac{\partial}{\partial z}\,\tilde{\phi}_r^e(\alpha,z)\Big|_{z=0-} \qquad (A.2b)$$

Likewise, continuity of H_ϕ and H_r at $z = 0$ and inspection of (A.1c) and (A.1d) give

$$n_1^2\,\tilde{\phi}_r^e(\alpha,0+) = n_2^2\,\tilde{\phi}_r^e(\alpha,0-) \qquad (A.2c)$$

$$\frac{\partial}{\partial z}\,\tilde{\phi}_r^m(\alpha,z)\Big|_{z=0+} = \frac{\partial}{\partial z}\,\tilde{\phi}_r^m(\alpha,z)\Big|_{z=0-} \qquad (A.2d)$$

A.3 Boundary and Source Conditions at the Source Plane

The continuity of E_ϕ and E_r at $z = z'$ and inspection of (A.1a) and (A.1b) yields

$$\tilde{\phi}^m_r(\alpha, z'+) = \tilde{\phi}^m_r(\alpha, z'-) \tag{A.3a}$$

$$\frac{\partial}{\partial z}\tilde{\phi}^e_r(\alpha, z)\Big|_{z=z'+} = \frac{\partial}{\partial z}\tilde{\phi}^e_r(\alpha, z)\Big|_{z=z'-} \tag{A.3b}$$

Using the fact that the magnetic intensity $\bar{H}$ must be discontinuous as the result of surface currents, while the electric flux density $\bar{D}$ must be discontinuous at points where surface charge accumulations exist, we find the additional expressions

$$\frac{\partial}{\partial z}\tilde{\phi}^m_r(\alpha, z)\Big|_{z=z'+} - \frac{\partial}{\partial z}\tilde{\phi}^m_r(\alpha, z)\Big|_{z=z'-} = -i\nu k_o J_\nu(k_o \alpha r') \tag{A.3c}$$

$$\tilde{\phi}^e_r(\alpha, z'+) - \tilde{\phi}^e_r(\alpha, z'-) = \frac{k_o^2 \zeta_o \alpha r'}{in_2^2} J'_\nu(k_o r' \alpha) \tag{A.3d}$$

Equations (A.2a) through (A.2d) and equations (A.3a) through (A.3b) constitute the independent set of eight equations we need in order to solve for the transform coefficients. Indeed, using (2.30a) and (2.30b) with (A.2a) through (A.2b) we find

$$A^m_r = \frac{2u_2}{u_1+u_2} B^m_{pr} \tag{A.4a}$$

$$B^m_{nr} = \frac{u_2-u_1}{u_2+u_1} B^m_{pr} \tag{A.4b}$$

$$A_r^e = \frac{2u_2n_2^2}{u_2n_1^2+u_1n_2^2} B_p^e \qquad (A.4c)$$

$$B_{nr}^e = \frac{u_2n_1^2-u_1n_2^2}{u_2n_1^2+u_1n_2^2} B_p^e \qquad (A.4d)$$

Likewise, using (2.30b) and (2.30c) with (A.3a) through (A.3d), we have

$$D_r^m = \left\{ \frac{u_2-u_1}{u_1+u_2} e^{k_o u_2 z'} + e^{-k_o u_2 z'} \right\} B_{pr}^m \qquad (A.3a)$$

$$D_r^e = \left\{ \frac{u_2n_1^2-u_1n_2^2}{u_2n_1^2+u_1n_2^2} e^{k_o u_2 z'} - e^{-k_o u_2 z'} \right\} B_{pr}^e \qquad (A.5b)$$

$$B_{pr}^m = \frac{i\gamma R_o k_o^2}{2u_2} J_\nu(k_o \alpha r') \qquad (A.5c)$$

$$B_{pr}^e = \frac{k_o^2 \zeta_o \alpha r'}{i2n_2^2} J_\nu'(k_o r' \alpha) \qquad (A.5d)$$

Since (A.4a) through (A.4d) and (A.5a) and (A.5b) are given in terms of either B_{pr}^m or B_{pr}^e, and since these are given explicitly by (A.5c) and (A.5d), respectively, the transform coefficients Φ_r^m and Φ_r^e are now known.

A.4 Integral Representations for Φ_r^e, Φ_r^m

Upon substitution of (A.4a) through (A.4d) and (A.5a) and (A.5b) into (2.30a) through (2.30c) we find

$$\tilde{\Phi}_r^e(\alpha,z) = B_{pr}^e \frac{2u_2n_2^2}{u_2n_1^2+u_1n_2^2} e^{-k_o(u_1 z - u_2 z')}, \quad z \geq 0 \qquad (A.6a)$$

$$\tilde{\Phi}_r^m(\alpha,z) = B_{pr}^m \frac{2u_2}{u_1+u_2} e^{-k_o(u_1 z - u_2 z')}, \quad z \geq 0 \tag{A.6b}$$

$$\tilde{\Phi}_r^e(\alpha,z) = B_{pr}^e \left\{ \frac{u_2 n_1^2 - u_1 n_2^2}{u_2 n_1^2 + u_1 n_2^2} e^{k_o u_2 (z+z')} + \text{sgn}[(z-z')] e^{-k_o u_2 |z-z'|} \right\}, \quad z \leq 0 \tag{A.6c}$$

$$\tilde{\Phi}_r^m(\alpha,z) = B_{pr}^m \left\{ \frac{u_2 - u_1}{u_2+u_1} e^{k_o u_2 (z+z')} + e^{-k_o u_2 |z-z'|} \right\}, \quad z \leq 0 \tag{A.6d}$$

where sgn[(z-z')] in (A.6c) is the numberical sign of (z-z').

With the field transforms thus specified, we may employ (2.10) directly in order to generate the required integral representations, thus

$$\Phi_r^e(r,z) = \frac{k_o^2 \zeta_o r'}{i 4 n_2^2} \int_{\infty e^{-i\pi}}^{\infty} J_\nu'(k_o \alpha r') H_\nu^{(2)}(k_o \alpha r) \frac{2u_2 n_2^2}{u_2 n_1^2 + u_1 n_2^2} e^{-k_o(u_1 z - u_2 z')} \alpha^2 d\alpha, \quad z \geq 0 \tag{A.7a}$$

$$\Phi_r^m(r,z) = \frac{i\gamma R_o k_o^2}{4} \int_{\infty e^{-i\pi}}^{\infty} J_\nu(k_o \alpha r') H_\nu(k_o \alpha r) \frac{2u_2}{u_1+u_2} e^{-k_o u_2 (z-z')} \frac{\alpha d\alpha}{u_2}, \quad z \geq 0 \tag{A.7b}$$

$$\phi_r^e(r,z) = \frac{k_0\zeta_0 r'}{i4n_2^2}\int_{\infty e^{-i\pi}}^{\infty} J_\nu'(k_0\alpha r')H_\nu^{(2)}(k_0\alpha r)$$

$$\left\{\frac{u_2n_1^2-u_1n_2^2}{u_2n_1^2+u_1n_2^2}\ e^{k_0u_2(z+z')} + \mathrm{sgn}[(z-z')]\ e^{-k_0u_2\ z-z'}\right\}\ \alpha^2 d\alpha$$

$$z \geq 0 \qquad \text{(A.7c)}$$

$$\phi_r^m(r,z) = \frac{i\gamma R_0 k_0^2}{2}\int_{\infty e^{-i\pi}}^{\infty} J_\nu(k_0\alpha r')H_\nu^{(2)}(k_0\alpha r)$$

$$\left\{\frac{u_2-u_1}{u_2+u_1}\ e^{k_0u_2(z+z')} + e^{-k_0u_2|z-z'|}\right\}\frac{\alpha d\alpha}{u_2}\ ,\quad z \leq 0 \qquad \text{(A.7d)}$$

Appendix B

The Steepest Descent Evaluation of V_e^s

To find the saddle-points of $q_2(s_2)$ in the s_2-plane we must evaluate $\frac{dq_2}{ds_2}$, and upon doing this we find

$$\frac{dq_2}{ds_2} = -\left[\frac{2\lambda s_2}{n_2^2 - s_2^2}\right] \tag{B.1}$$

From (B.1) we conclude that $s_2 = 0$ is a saddle-point for $q_2(s_2)$. Further analysis shows that for Im $n_2 \ll 1$ (as we assume), the path of steepest descent is essentially along the Re s_2 axis.

Differentiation of (B.1) provides

$$\left.\frac{d^2 q_2}{ds_2^2}\right|_{s_2=0} = \frac{-2\lambda_2}{n_2^2} \tag{B.2}$$

Notice that since λ is an even function of s_2, then $q(s_2)$ is an even function of s_2, so the coefficient of the s_2^3 term in a Taylor series must vanish, thus

$$\frac{d^3 q_2}{ds_2^3} = 0 \tag{B.3}$$

A Taylor series representation of $q(s_2)$ through the first four terms about $s_2 = 0$ is thus, using (B.1), (B.2), and (B.3),

$$q_2(s_2) = q_2(0) - \frac{\lambda 2}{n_2^2}\, s_2^2 \tag{B.4a}$$

where

$$q_2(0) = 2\left\{\lambda_2 + \frac{\gamma}{2}\log\ \frac{\gamma-\lambda_2}{\gamma+\lambda_2}\right\} \tag{B.4b}$$

Consider now γ_e for $z \leq 0$ as given by (3.22c). If we let $u_2 = is_2$, then

$$\gamma_e(y,y',z,z';s_2) = \frac{e^{k_o\lambda(y+y')}}{\lambda}\left\{\frac{is_2n_1^2-u_1n_2^2}{is_2n_1^2+u_1n_2^2}\ e^{ik_o(z+z')s_2}\right.$$

$$\left. + e^{-ik_o|z-z'|s_2}\right\} \tag{B.5}$$

Consideration of (B.5) for $s_2 = 0$ yields

$$\gamma_e(y,y',z,z';0) = 0 \tag{B.6}$$

so we must evaluate

$$\left.\frac{\partial^2\gamma_e}{\partial s_2^2}\right|_{s_2=0}$$

in order to generate the leading term in the asymptotic expansion of V_e^s. Doing this, we find

$$\left.\frac{\partial^2 \gamma_e}{s_2^2}\right|_{s_2=0} = 4\,\frac{e^{k_o(y+y')(\gamma^2-n_2^2)^{1/2}}}{(\gamma^2-n_2^2)^{1/2}}\left[k_o z' - \frac{n_1^2}{n_2^2(n_2^2-n_1^2)^{1/2}}\right]$$

$$\left[k_o z - \frac{n_1^2}{n_2^2(n_2^2-n_1^2)^{1/2}}\right] \qquad (B.7)$$

The leading term of the asymptotic expansion of V_e^s has the form (cf. [10])

$$V_e^s(y,y',z,z') \sim \frac{-\zeta_o}{8\pi n_2^2 k_o R_o}\, e^{k_o R_o q_2^{(0)}} \left[\left.\frac{\partial^2 \gamma_e}{s_2^2}\right|_{s_2=0}\right] \int_0^\infty e^{-k_o R_o\left(\frac{\lambda_2}{n_2^2}\right)s_2^2} s_2^2 ds_2 \qquad (B.8)$$

Using

$$\int_0^\infty e^{-k_o R_o\left(\frac{\lambda_2}{n_2^2}\right)s_2^2} s_2^2 ds_2 = \left(\frac{n_2^2}{\lambda_2 k_o R_o}\right)^{3/2} \frac{\sqrt{\pi}}{8}$$

and (B.7) in (B.8),

$$V_e^s(y,y',z,z') \sim \frac{-\zeta_o}{16\pi^2 n_2^2 k_o R_o}\left(\frac{\pi n_2^2}{\lambda_2 k_o R_o}\right)^{3/2} e^{k_o R_o q_2^{(0)}} \frac{e^{k_o\lambda_2(y+y')}}{\lambda_2}\left[k_o z' - \frac{n_1^2}{n_2^2(n_2^2-n_1^2)^{1/2}}\right]\left[k_o z - \frac{n_1^2}{n_2^2(n_2^2-n_1^2)^{1/2}}\right] \qquad (B.9)$$

which is (3.23) in Section 3.3.2.

Appendix C

The Evaluation of P and C

C.1. The Evaluation of P

Application of (1.3) to the channel guide cross section in Figure 4.1 gives

$$P = 2 \int_{-d}^{o} dx \int_{o}^{b} dy(E_{ox}H_{ow}) \tag{C.1}$$

Our consideration of modes far from cutoff manifests itself in (C.1) in that the integration can be taken over the guide cross section only. Substitution of (4.2b) and (4.2f) in (c.1) yields

$$P = -2A^2 \frac{n^2k_o^2-k_x^2}{k_x^2} \frac{k_o n^2}{\beta\xi_o} \int_{-d}^{o} \sin^2[k_x(x+\xi)]dx \int_{o}^{b} \cos^2[k_w(w+\eta)]dw \tag{C.2}$$

Expansion of the integrand in $\int_{-d}^{o} \sin^2[k_x(x+\xi)]dx$ and use of (D.7a), (D.7b), (D.9a), and (D.9b) [cf. Appendix D] gives

$$\int_{-d}^{o} \sin^2 k_x(x+\xi)dx = \frac{d}{2} + \frac{n^2}{2} \left\{ \frac{n_1^2\gamma_3}{(n^4\gamma_3^2+n_1^4k_x^2} + \frac{n_2^2\gamma_2}{(n^4\gamma_2^2+n_2^4k_x^2)} \right\} \tag{C.3}$$

Similarly, expansion of the integrand of $\cos^2[k_w(w+\eta)]dw$ and use of (D.4a), (D.4b), (D.6a), and (D.6b) gives

$$\int_{o}^{b} \cos^2 k_w(w+\eta)dw = \frac{b}{2} + \frac{\gamma_4}{k_o^2(n^2-n_2^2)} \tag{C.4}$$

Making the definitions

$$L_x \triangleq \frac{n^2}{2}\left\{\frac{n_1^2\gamma_3}{(n^4\gamma_3^2+n_1^4k_x^2}+\frac{n_2^2\gamma_2}{(n^4\gamma_2^2+n_2^4k_x^2)}\right\} \tag{C.5a}$$

$$L_w \triangleq \frac{\gamma_4}{k_o^2(n^2-n_2^2)} \tag{C.5b}$$

and substituting (C.3) and (C.4) into (C.2) gives

$$P = -2A^2\left[\frac{n^2k_o^2-k_x^2}{k_x^2}\right]\left[\frac{k_on^2}{\beta\zeta_o}\right]\left(\frac{d}{2}+L_x\right)\left(\frac{b}{2}+L_w\right) \tag{C.6}$$

C.2. The Evaluation of C

C.2.1 An Explicit Integral Representation of C

For the circumstance of modes far from cutoff, $\beta \approx (n^2k_o^2-k_x^2)^{1/2} \approx nk_o$, thus from (4.2a) and (4.2b) we have $|E_{ox}/E_{os}| \approx \beta/k_x >> 1$, thus we will neglect E_{os} as a field source and consider our straight guide modes to have only x-directed components. Recalling (2.49), where $E_{or} \rightarrow E_{ow}$ (i.e., E_{or} becomes E_{ow} in our local coordinate system for the straight guide , $E_{oq} \rightarrow E_{os}$, and $E_{oz} \rightarrow E_{ox}$, we conclude that for the special case we are now addressing $\phi^m(x,w) = 0$ or, in particular

$$\phi_s^m(x,w) = 0 \tag{C.7}$$

Rewriting (1.4) in terms of the local coordinates of the straight guide,

$$C = \int_{-d}^{0}\{\bar{E}_o^- x\delta\bar{H} - \delta\bar{E}x\bar{H}_o^-\} \cdot \bar{a}_w dx\Big|_{x=b} \tag{C.8}$$

The straight guide fields $\bar{E}_o$ and $\bar{H}_o$ can be written in the form

$$\bar{E}_o = E_{ox}\bar{a}_x \tag{C.9a}$$

$$\bar{H}_o = -H_{ow}\bar{a}_w + H_{os}\bar{a}_s \tag{C.9b}$$

Because of the scalar product with $\bar{a}_w$ that occurs in (C.8) and the forms of $\bar{E}_o$ and $\bar{H}_o$, we conclude that we need only find the components δE_x of $\delta\bar{E}$ and δH_s of $\delta\bar{H}$ in order to evaluate C.

Using (C.7) in (1.5c) and recalling that we have defined $\phi^e = E_x$ and $\phi^m = H_x$ (where the subscript z becomes x and the subscript ϕ becomes s in our local coordinate system) we have

$$k_o^2 n_2^2 H_\delta^s = i\omega\varepsilon \frac{\partial \phi_s^e}{\partial r} - e^{i\nu\phi}\int_0^\infty \left(\frac{\partial^2 \tilde{H}_\delta^s}{\partial z^2}\right) J_\nu(k_o\alpha r)\alpha d\alpha \tag{C.10}$$

where we have inserted the Hankel Transform representation of H_δ^s. Substituting $\tilde{H}_\delta^s$ from (1.10c) in C.10) gives

$$k_o^2 n_2^2 H_\delta^s = i\omega\varepsilon \frac{\partial \phi_s^e}{\partial r} + i\frac{n_2^2}{\zeta_o}\int_0^\infty \frac{\partial^2 \tilde{\phi}_s^e}{\partial z^2} J_\nu(k_o\alpha r)d\alpha \tag{C.11}$$

However, since from (3.23) we see that V_e^s is linear in z, it follows from (2.49) that $\frac{\partial^2 \phi_s^e}{\partial z^2} \equiv 0$, thus $\frac{\partial^2 \tilde{\phi}_s^e}{\partial z^2} \equiv 0$, and (C.11) becomes

$$H_\delta^s = \frac{-i}{\zeta_o k_o}\frac{\partial}{\partial w}\phi_s^e(x,w) \tag{C.12}$$

where we have used $\frac{\partial}{\partial r} = \frac{\partial}{\partial y} = \frac{\partial}{\partial w}$.

If we now substitute (4.1) into (3.23) we see that

$$\frac{\partial \Phi_s^e}{\partial w} = \lambda_2 k_o \Phi_s^e(x,w) \tag{C.13}$$

so use of (C.13) in (C.12) yields

$$H_\delta^s \triangleq \delta H_\delta = \frac{-i\lambda_2}{\zeta_o} \Phi_s^e(x,w) \tag{C.14}$$

With (C.9a), (C.9b), and (C.14) we find the following:

$$\bar{E}_o^- x \delta\bar{H} \cdot \bar{a}_w = \frac{i\lambda_2}{\zeta_o} \Phi_s^e(x,w)\ E_{ox}(x,w) \tag{C.15}$$

$$\delta\bar{E} x \bar{H}_o \cdot \bar{a}_w = - \Phi_s^e(x,w) H_{o\delta}(x,w) \tag{C.16}$$

Substitution of (C.15) and (C.16) in (C.8) yields

$$C = \int_{-d}^{o} \Phi_s^e(x,w) \left\{ \left(\frac{i\lambda_2}{\zeta_o} \right) E_{ox}(x,w) + H_{o\delta}(x,w) \right\} dx \Bigg|_{w=b} \tag{C.17}$$

Finally, we can use (4.2b) and (4.2d) in (C.17) to generate the expression

$$C = - \int_{-d}^{o} \Phi_s^e(x,b) \left\{ \frac{A}{\zeta_o} \left[\frac{n^2 k_o^2 - k_x^2}{\beta} \left(\frac{\lambda_2}{k_x} \right) \cos k_w(b+\eta) + \frac{n^2 k_o}{\beta} \left(\frac{k_w}{k_x} \right) \sin k_w(b+\eta) \right] \sin k_x(x+\xi) \right\} dx \tag{C.18}$$

C.2.2 An Explicit Representation of $\Phi_s^e(x,w)$

Having (C.18), our objective becomes that of finding an explicit form of $\Phi_s^e(x,w)$ for the special case under consideration. We begin by rewriting (3.23) in the abbreviated form (in terms of local coordinates)

$$V_s^e(w,w',x,x') = C_o V_e^s(w,w') u_e^s(x,x') \tag{C.19a}$$

where

$$C_o \triangleq \frac{-\zeta_o}{16\pi^2 n_2^2 k_o R_o} \left(\frac{\pi n_2^2}{\lambda_2 k_o R_o}\right)^{3/2} \frac{e^{k_o R_o q_2(0)}}{\lambda_2} \tag{C.19b}$$

$$V_e^s(w,w') \triangleq e^{k_o\lambda_2(w-b/2)} \; e^{k_o\lambda_2(w'-b/2)} \tag{C.19c}$$

$$u_e^s(x,x') \triangleq (k_o x' - \underline{k}) \; (k_o x - \underline{k}) \tag{C.19d}$$

where

$$K \triangleq \frac{n_I^2}{n_2^2(n_2^2-n_1^2)^{1/2}} \tag{C.19e}$$

Upon substitution of (C.19a) and (4.2b) into (2.64) we find

$$\Phi_s^e(w,x) = -AC_o w(n^2-n_2^2) R_o \left(k_2^2 + \frac{\partial^2}{\partial x^2}\right) \frac{n^2k_o^2-k_x^2}{\beta k_x}$$
$$\int_o^b V_e^s(w,w') \cos k_w(w'+\eta) dw' \int_{-d}^{o} u_e^s(x,x') \sin k_x(x'+\xi) dx' \tag{C.20}$$

The integral on [0,b] in (C.20) becomes, upon inserting (C.19c),

$$\int_o^b V_e^s(w,w') \cos k_w(w'+\eta) dw' =$$
$$e^{k_o\lambda_2(w-\frac{b}{2})} \int_o^b e^{k_o\lambda_2(w'-b/2)} \cos k_w(w'+\eta) dw' \tag{C.21}$$

Carrying out the integration on the RHS of (C.21) and using (D-4a), (D-4b), (D-6a), and (D-6b) yields

$$C_1 \triangleq \int_o^b e^{k_o\lambda_2(w'-b/2)} \cos k_w(w'+\eta)dw' =$$

$$\frac{k_w}{k_o\gamma_2^2(n^2-n_2^2)^{1/2}} \left\{ \lambda_2 k_o \left[\mathrm{sgn}[\cos(k_w b)]\ \mathrm{sgn}[k_w^2-\gamma_4^2] \right.\right.$$

$$\left. e^{(k_o b\lambda_2)/2} - e^{-(k_o b\lambda_2)/2} \right] + \gamma_4 \left[\mathrm{sgn}[\cos(k_w b)] \right.$$

$$\left.\left. \mathrm{sgn}[k_w^2-\gamma_4^2]\ e^{(k_o b\lambda_2)/2} + e^{-(k_o b\lambda_2)/2} \right] \right\} \qquad \text{(C.22)}$$

Combining (C.22) with (C.21) we have

$$\int_o^b V_e^s(w,w') \cos k_w(w'+\eta)dw = C_1\, e^{k_0\lambda_2(w-\frac{b}{2})} \qquad \text{(C.23)}$$

The integral on [-d,0] in (C.20) becomes, upon inserting (C.19d),

$$\int_{-d}^o u_e^s(w,w') \sin k_x(x'+\xi)dx' =$$

$$(k_o x-\underline{k}) \int_{-d}^o (k_o x'-\underline{k}) \sin k_x(x'+\xi)dx' \qquad \text{(C.24)}$$

Evaluating the integral on the RHS of (C.24) and using (D-7a), (D-7b), (4.6a), and (4.6b) we find

$$C_2 \triangleq \int_{-d}^o (k_o x'-\underline{k}) \sin k_x(x'+\xi)dx' = \left\{ \frac{k_o}{k_x} \right.$$

$$\left[\mathrm{sgn}\ [\cos(k_x d)]\ \mathrm{sgn}\ [n_1^2 n_2^2 k_x^2 - n^4\gamma_2\gamma_3] \right. \frac{(n^2\gamma_2 d+n_2^2)}{(n_2^4 k_x+n^4\gamma_2^2)^{1/2}}$$

$$- \frac{n_1^2}{(n^4\gamma_3^2+n_1^4k_x^2)^{1/2}}\Bigg] + \frac{K_n^2}{k_x}\Bigg[\frac{\gamma_3}{(n^4\gamma_3^2+n_1^4k_x^2)^{1/2}}$$

$$+ \text{sgn}\,[\cos(k_x d)]\ \text{sgn}\,[n_1^2n_2^2k_x^2-n^4\gamma_2\gamma_3]\ \frac{\gamma_2}{(n_2^4k_x^2+n^4\gamma_2^2)^{1/2}}\Bigg]\Bigg\} \quad \text{(C.25)}$$

Combining (C.25) with (C.24) we have

$$\int_{-d}^{o} u_e^s(x,x')\ \sin k_x(x'+\zeta)dx' = C_2\ (k_o x - k) \quad \text{(C.26)}$$

We can now employ (C.19b), (C.23), and (C.26) with (C.20) to produce the result

$$\phi_s^e(w,x) = \Bigg\{ AC_1C_2\ \frac{k_o^2(n^2-n_2^2)\ (n^2k_o^2-k_x^2)}{16\pi^2\beta k_x\lambda_2}$$

$$\left(\frac{\pi n_2^2}{k_o R_o \lambda_2}\right)^{3/2}\ e^{k_o\lambda_2(w-\frac{b}{2})}\ e^{k_o R_o q_2(0)}\ (k_o x-k)\Bigg\} \quad \text{(C.27)}$$

where we have also used $w\varepsilon_o = \frac{k_o}{\zeta_o}$.

C.2.3 An Explicit Representation of C

Having (C.27), we need only use it with (C.18) to obtain

$$C = \Bigg\{-A^2C_1C_2^2\ \text{sgn}\,[\cos(k_w b)]\ \text{sgn}\,[k_w^2-\gamma_4^2]$$

$$\frac{k_w k_o (n^2k_o^2-k_x^2)(n^2-n_2^2)^{1/2}}{16\pi^2\beta^2k_x^2\lambda_2\zeta_o}\ \left[\lambda_2(n^2k_o^2-k_x^2) + n^2k_o\gamma_4\right]$$

$$\left(\frac{\pi n_2^2}{k_o R_o \lambda_2}\right)^{3/2}\ e^{(k_o\lambda_2 b)/2}\ e^{k_o R_o q_2(0)}\Bigg\} \quad \text{(C.28)}$$

APPENDIX D

THE EXPLICIT REPRESENTATION OF TRIGONOMETRIC FUNCTIONS IN TERMS OF PROBLEM PARAMETERS

During the course of the analysis in Appendix C we employ a set of identities which express trigonometric functions explicitly in terms of the eigenvalues K_x, K_w and the material parameters of our problem. The development of these identities from equations (4.4a), (4.4b), (4.6a), and (4.6b) is a straightforward arithmetical procedure, but one must exercise care in accounting for a multitude of possible choices of numerical sign if ambiguous results are to be avoided.

Consideration of (4.4a) and (4.4b) reveals that the eigenvalues K_x, K_w may be either less than or greater than zero. Indeed, review of the field expressions (4.2a) through (4.2f) shows that the numerical signs of K_x and K_w don't effect these formulae at all; i.e., the field expressions depend on $|K_x|$ and $|K_w|$. We are thus free to choose the numerical signs of K_x and K_w and will choose these to be the positive solutions of the eigenvalue equations (4.4a) and (4.b).

Consider now equations (4.6a) and (4.6b). Since we choose $K_x > 0$ and $K_w > 0$, and since $\gamma_3 > 0$ and $\gamma_4 > 0$, we can always find solutions ξ and η such that

$$\frac{-\pi}{2K_x} < \xi < 0 \qquad \text{(D.1a)}$$

$$\frac{-\pi}{2K_w} < \eta < 0 \tag{D.1b}$$

Choosing ξ and η as in (D.1a) and (D.1b), respectively we have

$$\sin(K_w\eta) < 0 \tag{D.2a}$$

$$\cos(K_w\eta) > 0 \tag{D.2b}$$

$$\sin(K_x\xi) < 0 \tag{D.2c}$$

$$\cos(K_x\xi) > 0 \tag{D.2d}$$

We can now proceed to outline the derivation of the identities we require in Appendix C.

Using the trigonometric identites

$$\sin\theta = \frac{\mathrm{sgn}[\cos\theta]\tan\theta}{(1+\tan^2\theta)^{\frac{1}{2}}} \tag{D.3a}$$

$$\cos\theta = \frac{\mathrm{sgn}[\cos\theta]}{(1+\tan^2\theta)^{\frac{1}{2}}} \tag{D.3b}$$

with (4.6b) and (D.2a), (D.2b), we find

$$\sin(K_w\eta) = -\frac{\gamma_4}{k_o(n^2 - n_2^2)^{\frac{1}{2}}} \tag{D.4a}$$

$$\cos(k_w\eta) = \frac{k_w}{k_o(n^2 - n_2^2)^{\frac{1}{2}}} \tag{D.4b}$$

Similarly, use of (4.4b) with (D.3a), (D.3b) gives

$$\sin(K_w b) = \frac{\mathrm{sgn}[\cos(K_w b)]\mathrm{sgn}[K_w^2 - \gamma_4^2](2K_w\gamma_4)}{k_o^2(n^2 - n_2^2)} \tag{D.5a}$$

$$\cos(K_w b) = \frac{\mathrm{sgn}[\cos(K_w b)]\,|K_w^2 - \gamma_4^2|}{k_o^2(n^2 - n_2^2)} \tag{D.5b}$$

The use of both (D.4a), (D.4b) and (D.5a), (D.5b) with the standard trigonometric identities for sines and cosines of angular sums yields

$$\sin[K_w(b+\eta)] = \mathrm{sgn}[\cos(K_w b)]\,\mathrm{sgn}[K_w^2 - \gamma_4^2]\,\frac{\gamma_4}{k_o(n^2 - n_2^2)^{\frac{1}{2}}} \tag{D.6a}$$

$$\cos[K_w(b+\eta)] = \mathrm{sgn}[\cos(K_w b)]\,\mathrm{sgn}[K_w^2 - \gamma_4^2]\,\frac{K_w}{k_o(n^2 - n_2^2)^{\frac{1}{2}}} \tag{D.6b}$$

Now, proceeding in a similar way, one employs (4.6a) with (D.3a), (D.3b) and (D.2c), (D.2d) to produce

$$\sin K_x\xi = \frac{-K_x n_1^2}{(n^4\gamma_3^2 + n_1^4 K_x^2)^{\frac{1}{2}}} \tag{D.7a}$$

$$\cos K_x\xi = \frac{\gamma_3 n^2}{(n^4\gamma_3^2 + n_1^4 K_x^2)} \tag{D.7b}$$

Using (D.3a) and (D.3b) with (4.4a) one finds

$$\sin(K_x d) = \frac{\mathrm{sgn}[\cos(K_x d)]\,\mathrm{sgn}[n^2{}_1 n_2^2 K_x^2 - n^4\gamma_2\gamma_3]\,n^2 K_x(n_1^2\gamma_2 + n_2^2\gamma_3)}{(n_1^4 K_x^2 + n^4\gamma_3^2)^{\frac{1}{2}}(n_2^4 K_x^2 + n^4\gamma_2^2)^{\frac{1}{2}}} \tag{D.8a}$$

$$\cos(K_x d) = \frac{\mathrm{sgn}[\cos(K_x d)]\,|n_1^2 n_2^2 K_x^2 - n^4\gamma_2\gamma_3|}{(n_1^4 K_x^2 + n^4\gamma_3^2)\,(n_2^4 K_x^2 + n^4\gamma_2^2)^{\frac{1}{2}}} \tag{D.8b}$$

Finally, use of (D.7a), (D.7b) and (D.8a), (D.8b) with the trigonometric formulae for angular sums and differences yields

$$\sin[K_x(\xi - d)] = \frac{-\,\mathrm{sgn}[\cos(K_x d)]\,\mathrm{sgn}[n_1^2 n_2^2 K_x^2 - n^4\gamma_2\gamma_3]\,n_2^2 K_x}{(n_2^4 K_x^2 + n^4\gamma_2^2)^{\frac{1}{2}}} \tag{D.9a}$$

$$\cos[K_x(\xi-d)] = \frac{-\,\mathrm{sgn}[\cos(K_x d)]\,\mathrm{sgn}\,[n_1^2 n_2^2 K_x^2 - n^4\gamma_2\gamma_3]n^2\gamma_2}{(n_2^4 K_x^2 + n^4\gamma_2^2)^{\frac{1}{2}}} \tag{D.9b}$$

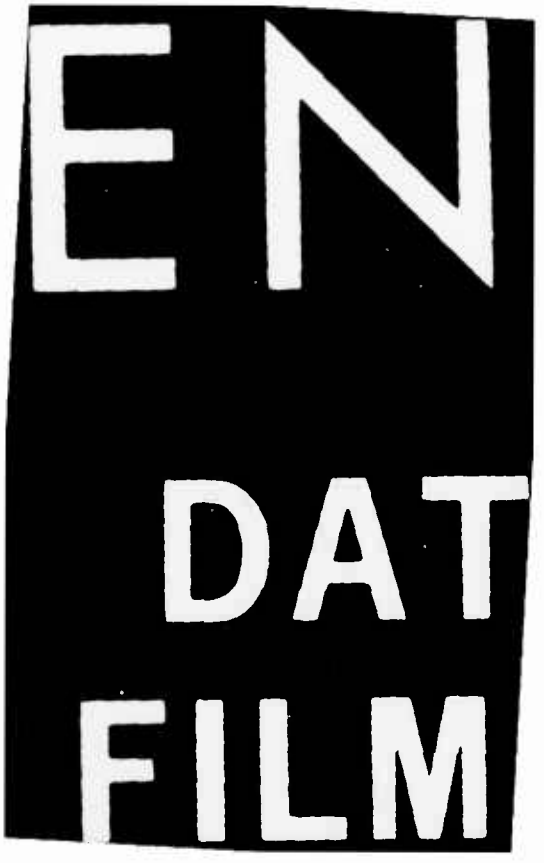
EN
DAT
FILM

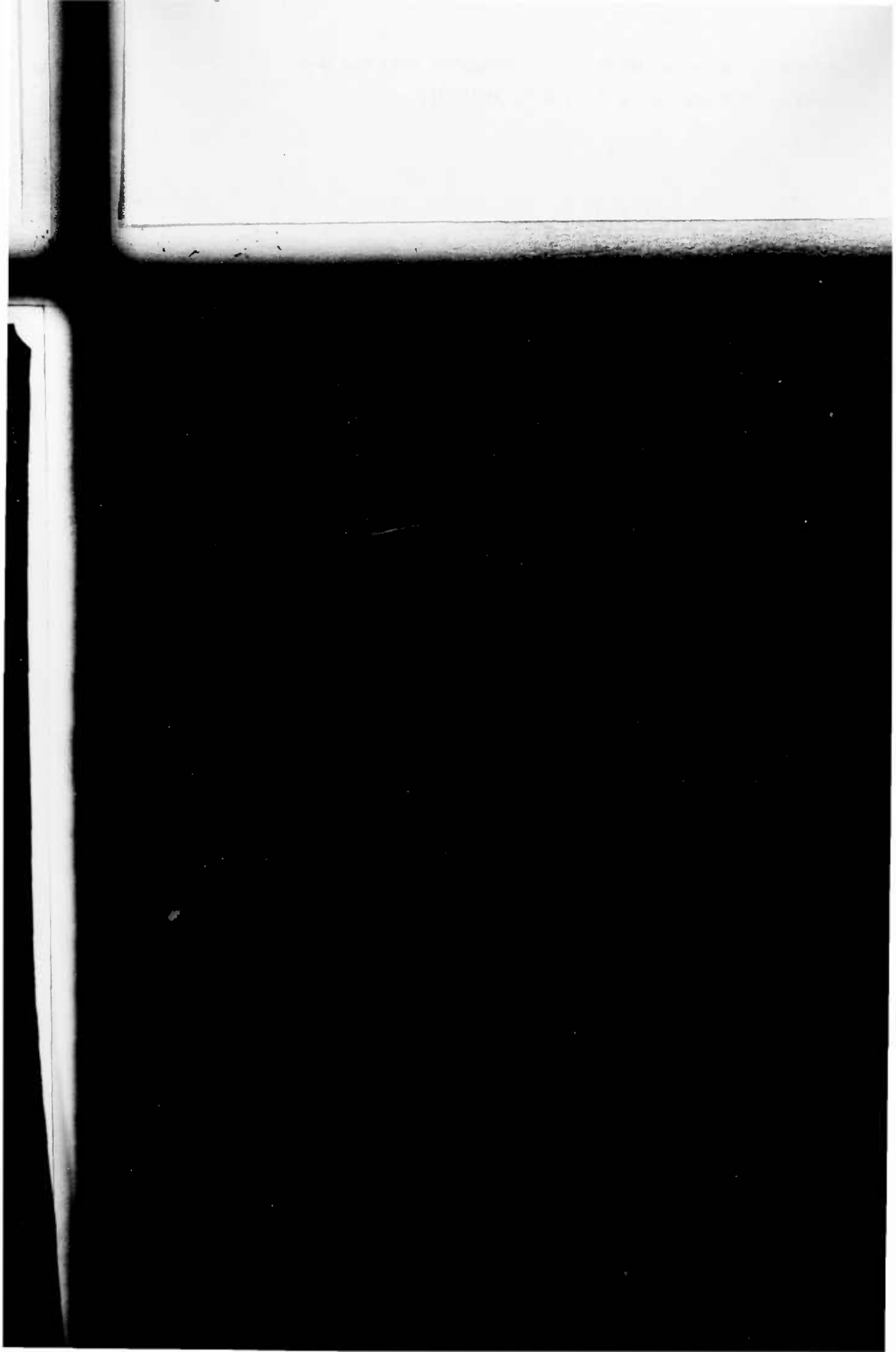

$$\frac{e^{k_o\lambda_2(y+y')}}{\lambda_2}\left[k_o z' - \frac{n_1^2}{n_2^2(n_2^2-n_1^2)^{1/2}}\right]\left[k_o z - \frac{n_1^2}{n_2^2(n_2^2-n_1^2)^{1/2}}\right] \qquad (B.9)$$

which is (3.23) in Section 3.3.2.

$$\int_0^b \cos^2 k_w(w+\eta)\,dw = \frac{b}{2} + \frac{\gamma_4}{k_0^2(n^2-n_2^2)} \qquad (C.4)$$

Rewriting (1.4) in terms of the local coordinates of the straight guide,

$$C = \int_{-d}^{0} \{\tilde{E}_0 \times \delta H - \delta E \times \tilde{H}_0\} \cdot \bar{a}_w dx \Big|_{x=b} \qquad (C.8)$$